Mechanistic Insight on the Stereoselective Photooxidation of Enecarbamates Using PTAD, a Singlet Oxygen Analog

A Thesis Presented

by

Catherine Cunneen Hooper

To the Joint Science Department

Of The Claremont Colleges

In partial fulfillment of

The degree of Bachelor of Arts

Senior Thesis in Chemistry

April 24, 2005

TABLE OF CONTENTS

List of Tables

Chapter 1

Chapter 3

List of Figures

Chapter 1

Chapter 4

List of Schemes

Chapter 1

List of Equations

Chapter 1:

Acknowledgments

I would like to first thank the Joint Science Department for all the opportunity and encouragement every faculty member has supplied me with during my time here at Claremont McKenna College. Any accomplishment of mine is more of a group effort, and all the credit goes to the people who make this institute for challenging me every step of the way, expecting me to live up to the highest expectations and helping me make my dreams come true over these past four years.

A most special thanks goes to my advisor Professor Thomas Poon, without whose patience, knowledge and ability to "put up with me" I would have never had such an opportunity to succeed. More than a mentor, Professor Poon's example has served as one of my main models of true work ethic and passion for that which one studies.

With the same respect, I would like to thank J. Sivaguru and Professor Turro of Columbia University for providing samples of the E-enecarbamates and fore the opportunity to join in this exciting project.

I would like to thank the whole Poon research group. All undergraduate members have become my closet friends and helped me get through the hard lab days. A special thanks to Professor Williams, the all knowing, who was always there to help me find the solution when I was lost in the lab. To Professor Black, for believing in me enough to let me take my crazy science schedules, and for giving me my love of O-Chem, Thank you. To professor Zanella, the one responsible for making me a chemistry major, thank you for making general chemistry so much easier to understand. I would also like to give a special thanks to Professor Corcoran whose patience and amazing passion for his own work has helped pushed me to do my best, especially in the actual writing of my thesis.

I would like to thank Sara Sorice, who has taught me what true unconditional love means and been there to catch me each time I fell. I would like to thank my whole family for their love and support, They are the ones who have given me the drive and confidence to achieve, the supporting phone conversations when I didn't think I could do it, and the pride that gives me everything to work for. I would like to especially thank my baby sister, my better half, Collette Hooper, for all the times she finished the experiments I could not get into lab to complete, for all her love, and for being my best role model. Last but definitely not least I would like to thank the woman of the Joint Science Faculty. Professor Hatcher-Skeers, Edwalds-Gilbert, Justice, Wiley and Tang are some of my greatest role models, supporters and friends. I strive to be as successful as each of you, balancing a family and career and still always happy.

And to my heavenly Lord, Jesus Christ, for blessing me with this life. "Bless the Lord, O my soul, and all that is within me, bless his holy name." -- Psalm 103:1

Thank You!

Abstract

Mechanistic Insight on Stereoselective Photooxidation of Enecarbamates Using PTAD, a Singlet Oxygen Analog

By Catherine Hooper

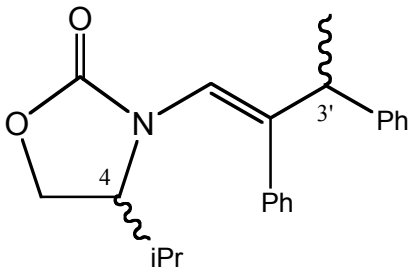

(Z4R,3'R/S)-**1a**
(Z4S,3'R/S)-**1b**

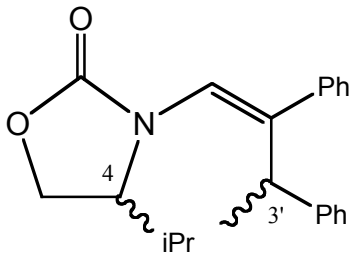

(E4R,3'R/S)-**1c**
(E4S,3'R/S)-**1d**

Stereoisomeric pairs of chiral oxazolidinone substituted enecarbamates **1a-1d** can be resolved using singlet molecular oxygen, the smallest known enophile. Resolution occurs via the selective reaction of singlet oxygen ($^1O_2$) with one of the diastereomers of the mixture (racemic at C-3') to form a dioxetane, which cleaves upon warming to yield one of the enantiomers of methyldesoxybenzoin (**MDB**) in up to 97% enantiomeric excess (e.e.). The explanation for this remarkable selectivity was, up to this point, thought to be due to steric hinderances, but is now suspected to involve either the deactivation of $^1O_2$ by C-H vibronic coupling via the isopropyl group of the oxazolidinone moiety or a directing effect from the carbonyl oxygen. 4-phenyl-1,2,4-triazoline-3,5-dione (PTAD), a highly reactive enophile with similar reactivity to $^1O_2$, has also been found to react stereoselectively with **1a-1d**, lending credence to the aforementioned processes. Comparing the reactivity and selectivity of PTAD and $^1O_2$ lends great mechanistic insight to the importance of vibrational deactivation of $^1O_2$ directing selectivity over steric factors. PTAD, a bulkier enophile than $^1O_2$, reacts with **1a-d** with little to no selectivity. This suggests that steric factors do not drive the unique selectivity of $^1O_2$, rather vibrational energy of C-H bonds of neighboring substituents to the double bond deactivate the excited molecule before it is able to react.

Abstract

Mechanistic Insight on Stereoselective Photooxidation of Enecarbamates Using PTAD, a Singlet Oxygen Analog

By Catherine Hooper

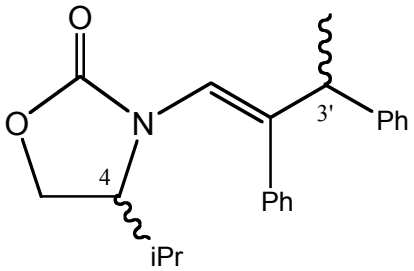

(Z4R,3'R/S)-**1a**
(Z4S,3'R/S)-**1b**

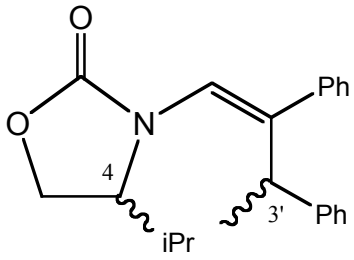

(E4R,3'R/S)-**1c**
(E4S,3'R/S)-**1d**

Stereoisomeric pairs of chiral oxazolidinone substituted enecarbamates **1a-1d** can be resolved using singlet molecular oxygen, the smallest known enophile. Resolution occurs via the selective reaction of singlet oxygen ($^1O_2$) with one of the diastereomers of the mixture (racemic at C-3') to form a dioxetane, which cleaves upon warming to yield one of the enantiomers of methyldesoxybenzoin (**MDB**) in up to 97% enantiomeric excess (e.e.). The explanation for this remarkable selectivity was, up to this point, thought to be due to steric hinderances, but is now suspected to involve either the deactivation of $^1O_2$ by C-H vibronic coupling via the isopropyl group of the oxazolidinone moiety or a directing effect from the carbonyl oxygen. 4-phenyl-1,2,4-triazoline-3,5-dione (PTAD), a highly reactive enophile with similar reactivity to $^1O_2$, has also been found to react stereoselectively with **1a-1d**, lending credence to the aforementioned processes. Comparing the reactivity and selectivity of PTAD and $^1O_2$ lends great mechanistic insight to the importance of vibrational deactivation of $^1O_2$ directing selectivity over steric factors. PTAD, a bulkier enophile than $^1O_2$, reacts with **1a-d** with little to no selectivity. This suggests that steric factors do not drive the unique selectivity of $^1O_2$, rather vibrational energy of C-H bonds of neighboring substituents to the double bond deactivate the excited molecule before it is able to react.

Chapter 1: Introduction

1.1 Singlet Oxygen.

Molecular Oxygen, O_2, is a molecule that is both vital and harmful to many living organisms. Its presence in our atmosphere is what makes our planet different from any other. Oxygen acts as the ultimate electron accepter in the electron transport chain, allowing metabolism to occur and providing life for every oxygen breathing organism.[1] On the other hand, oxygen is also responsible for the spoiling of food and rusting of metal, all due to the fact that this reactive molecule acts as a strong oxidizing agent.[2] Excited forms of oxygen, such as singlet oxygen, also play an important role in metabolic processes. Singlet molecular oxygen is the smallest known enophile.[3] Oxygen can be excited to its singlet state through various processes.[1] Specifically, this can be accomplished through direct irradiation, enzymatically by action of peroxidases or lipoxigenases, or by energy absorption from other molecules (photosensitizers).[4] When singlet oxygen is produced in living organisms it can attack cellular structures by oxidation of important cellular components like cell membranes or proteins. If an accumulation of the oxidative damage exceeds a certain threshold level it will cause cell death.[2] In photodynamic therapy for example, with the popular photosensitizer photofrin, singlet oxygen causes cell death by reacting with DNA.[3]

The oxidative degeneration of DNA is caused through two different mechanisms. The first is the transfer of electrons from photomutagenic and photocarcinogenic agents to the guanine base of DNA. The second is the transfer of energy from photosensitizer drugs to activate ground state oxygen to singlet oxygen, which will then cause damage by

oxidizing the same guanine sight on the DNA.[5] Through these modes of action scientists have found ways of using singlet oxygen in cancer therapy. This is but one example of the significance of $^1O_2$, which provides the impetus for exploring the reactivity of this fascinating molecular species.

1.2 Description of Singlet Oxygen.

Although often represented, via the Lewis structure, as two oxygen molecules joined by a double bond (Figure 1.1), the activity of molecular oxygen can be better understood by the structure presented in Figure 1.2.

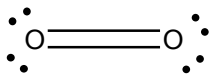

Figure 1.1. Lewis structure of molecular oxygen

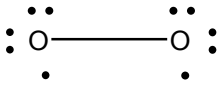

Figure 1.2. Representation of molecular oxygen in terms of reactivity

Quantum theory of atomic and molecular structure can be used to describe the excited state of this diatomic molecule. Ground state oxygen exists in the triplet state. This means the two unpaired valence electrons occupy the π_g^+ and π_g^- orbitals. In the first excited state of oxygen, also known as the singlet state, the two electrons in the π_g orbital will pair up and observe opposite spins while occupying either the π_g^+ or π_g^- together.[5] The molecular orbitals for both the possible ground states and excited states are shown below in Figures 1.3 and 1.4 respectively.

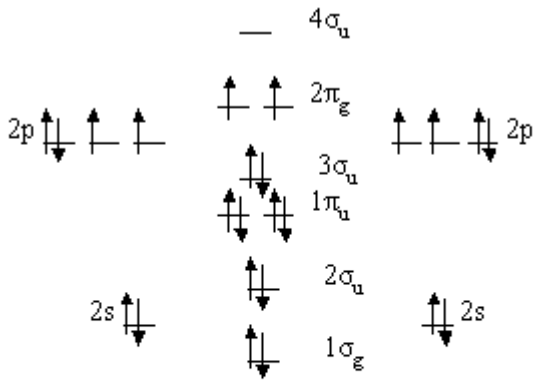

Figure 1.3. Molecular orbitals for ground state oxygen

Figure 1.4. $2\pi_g$ molecular orbitals for excited singlet state oxygen (Σ and Δ are electronic state designation that also indicate the value of orbital angular momentum on the molecular axis of the species)

The ($^1\Delta_g$) singlet state exists only 94 kJ mol^{-1} above the ground state triplet and is the lowest excited state. The transition to the $^3\Sigma_g^-$ ground state is strictly forbidden for the isolated $^1O_2$ ($^1\Delta_g$) molecule and only occurs through the excitation energy of 94 kJ mol^{-1} along with its empty $2\pi_g$ orbital causing singlet oxygen to be extraordinarily reactive.[7]

Varying vibrational deactivations of solvents and mediums in which singlet oxygen exists cause the lifetime of the excited molecule to have enormous solvent

dependence. The shortest lifetime is observed to be 3.1μs in H_2O and the longest 300ms in perfluorodecaline.[7] However, this time frame is still long enough for the $^1O_2$ to react with other molecular species.

As Figure 1.4 shows, the singlet state allows the two outer electrons to exist in either the π_g^+ or π_g^- orbitals. The Lewis structure below, drawn more as a zwitterion, demonstrates what this excited state means in terms of reactivity of the molecule (Figure 1.5).

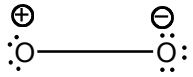

Figure 1.5. Lewis structure of excited oxygen

1.3 Reaction Mechanisms of Singlet Oxygen.

The discovery of the different factors affecting the stereoselectivity of singlet oxygen reactions has made possible the assessment of the mechanism in which singlet oxygen reacts with different molecules. Singlet oxygen is capable of performing the following pericyclic reactions: the Diels-Alder cycloaddition reaction,[8] [2 + 2] cycloadditions, and ene reactions with olefins (Scheme 1.1).[9] The [2 + 2] cycloaddition and ene reaction are most applicable to this study.

Scheme 1.1. Reactions with $^1O_2$.

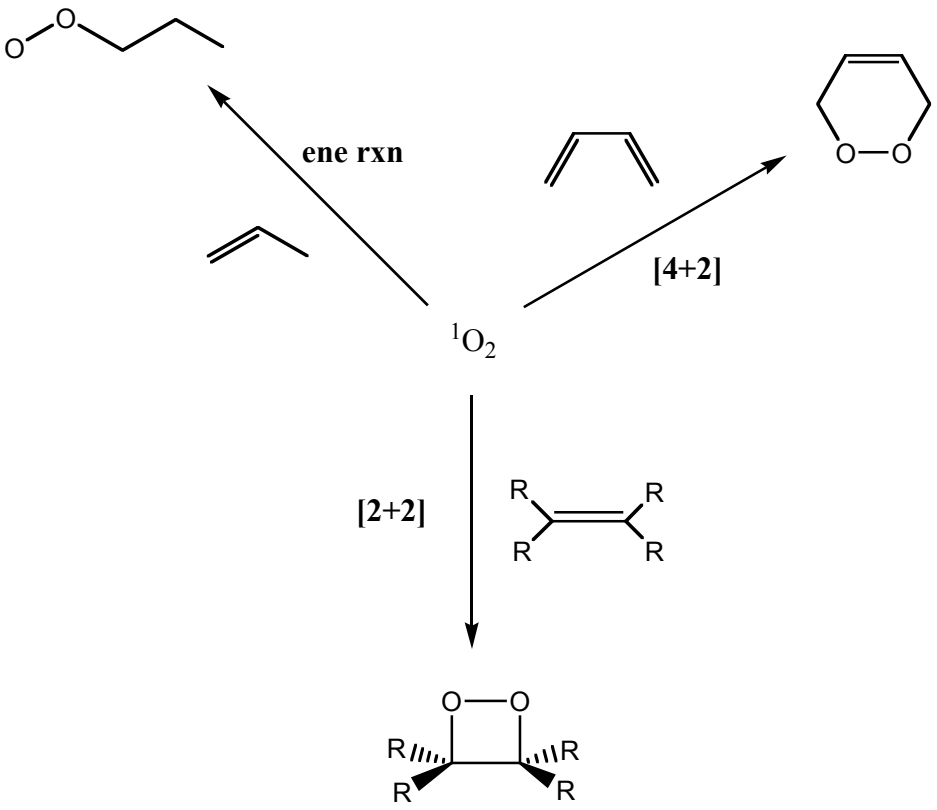

Understanding of this basic mechanism provides the foundation to singlet oxygen reactions. Past research has shown evidence that all three pericyclic reactions of $^1O_2$ (ene addition, [4 +2] cycloaddition and [2 + 2] cycloaddition) proceed through a structural perepoxide intermediate.[10,11]

It has been determined that the substituents on either side of the double bond play a large role in both the reaction rate and diastereoselecitvity of these reactions and are attributed to hydrogen directing effects. Intermediates of $^1O_2$ reactions are oriented such that a perpendicular attack of the oxygen molecule is driving the selectivity of the products.[12] Interaction between the δ^- oxygen and the adjacent hydrogen stabilizes the interaction of the δ^+ oxygen atom with the double bond. This can be referred to as the hydrogen steering complex. A strong preference is observed for allylic hydrogen

abstraction from the more crowded side of an alkene. This is known as the *cis*-effect. Figures 1.6.1 and 1.6.2 show comparable stabilized intermediates that demonstrate the hydrogen steering complex and the role played by substituents on either side of the double bond.[9,11]

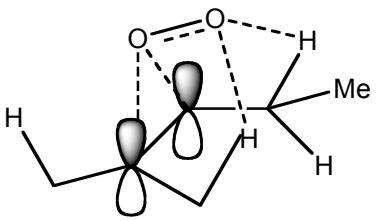

Figure 1.6.1: The $^1O_2$ is guided into the double bond with the support of two different electrostatic "hydrogen steering" interactions. This is the more stabilized intermediate and major products arise from H-abstraction on the more crowded side of the alkene.

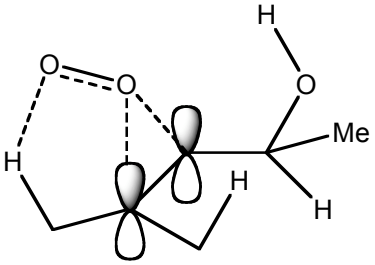

Figure 1.6.2. The $^1O_2$ undergoes a electrostatic interaction in which only one hydrogen is able to participate in the "hydrogen steering" that stabilizes this intermediate. This is the less stabilized intermediate due to little or no H-abstraction here.

1.4. Oxazolidinone-Substituted Chiral Enecarbamates and their reactions with $^1O_2$.

"Oxazolidinone-substituted chiral enecarbamates are mechanistically versatile systems for the study of conformational, electronic, stereoselectronic and steric effects on the stereoselectivity of oxidation reactions at the alkene functionality."[13] As shown in Figure 1.7 below, the forms of the E and Z isomers will be described from this point on as **1a**, **1b**, **1c**, and **1d**.

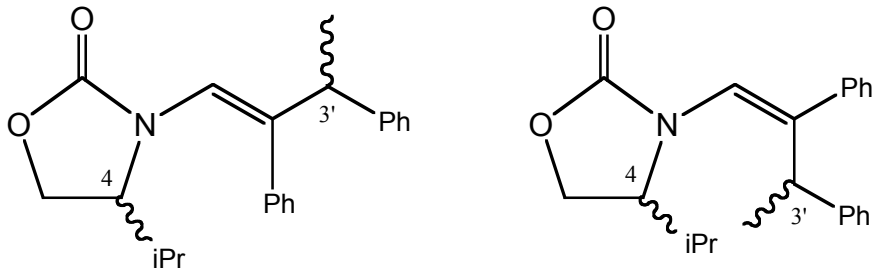

(Z4R,3'R/S)-**1a**
(Z4S,3'R/S)-**1b**

(E4R,3'R/S)-**1c**
(E4S,3'R/S)-**1d**

Figure 1.7. Oxazolidinone substituted enecarbamates (Z and E-isomers respectively) with chiral C-4 and C-3' centers.

Since oxazolidinones can be synthesized as optically pure chiral auxiliaries, they serve as perfect compounds with which to examine the role of stereocenters (in particular the C-3' stereocenter) in directing the attack of $^1O_2$. The general reaction of singlet oxygen with the enecarbamates proceeds as shown below in Scheme 1.2.[14] The factors, focusing on the C-3' chiral center, which cause the $^1O_2$ selectivity are of particular interest.

Scheme 1.2. Reaction of Singlet Oxygen with **1a**, the Z-4R,3'R/S epimeric pair of oxazolidinone substituted enecarbamates.

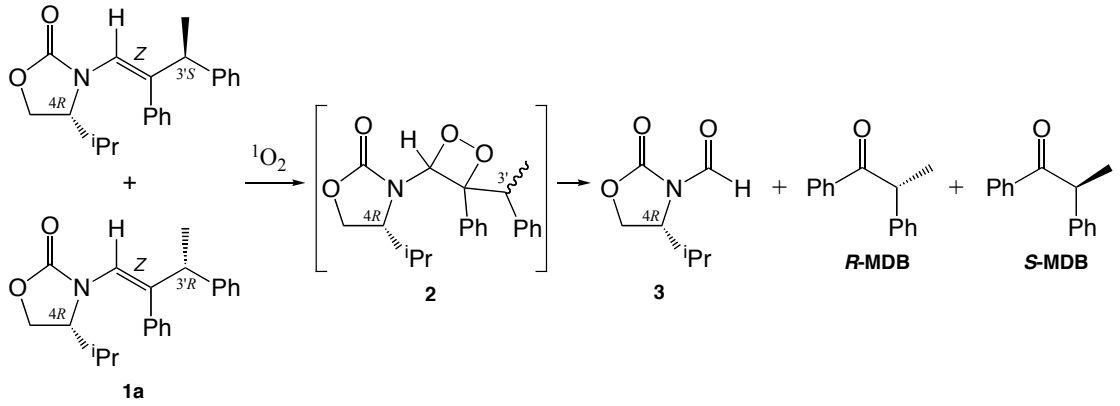

It was found that the dioxetane, **2**, was formed by the attack of $^1O_2$ from the face anti to the isopropyl substituent on the oxazolidinone ring.[13,14] On top of this, it is

important to note that the intermediate step before the dioxetane is produced is predicted to be an electrostatic interaction similar to that of the hydrogen steering presented in Section 1.3. In the case of this enecarbamate however, it is a complex with the oxygen (or alternatively the nitrogen) in the oxazolidinone ring that performs the electrostatic directing. This is shown below in Figure 1.8.1 and 1.8.2.

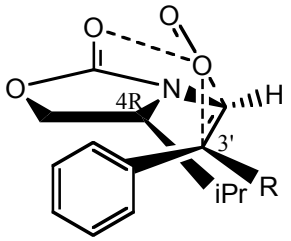

Figure 1.8.1. Transition state in which $^1O_2$ reacts with the enecarbamate adding perpendicular to the double bond.

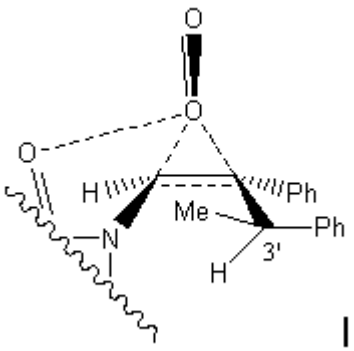

Figure 1.8.2. A second view of $^1O_2$ forming a complex with neighboring carbonyl oxygen when adding perpendicular to bond.

As reported in previous research, when the reaction shown in Scheme 1.2 is run with controlled chirality at C-4, selectivity in the products is observed.[13,14] "The rate of addition is further governed by the configuration of the chirality center at the C-3' position of the alkenyl side chain, such that partial conversion of **1a** (Scheme 1.2) affords nonracemic methldesoxybenzoin (MDB, scheme 1.2)."[14] The research done in this paper focuses on the effects of the chirality at the C-3' center. The stereoselectivity of attack by $^1O_2$ is dependent on a variety of factors such as temperature, solvent, and substrate

geometry, which when utilized in the correct combination, can yield MDB e.e.'s as high as 97%.[13]

A general sum of the results from this previous work is shown in Table 1.1.[14] The solvent for these reactions was $CDCl_3$. In order to show diastereoselectivity, the reactions were run to less than 100% completion (the limiting reagent in this case is the singlet oxygen).

Before proceeding, it is important to mention, the relationship between stereoselectivity of one enantiomer over another and rate of reaction. If an enantiomer or diastereomer provides a better physical orientation for singlet oxygen to attack the double bond, that specific stereoisomer will preferentially react with the singlet oxygen. This will cause a faster disappearance of that stereoisomer. On the other hand, if the enantiomer or diastereomer provides a physical orientation that causes quenching of the singlet oxygen, it will have less opportunity to react with $^1O_2$ causing a slower disappearance of that stereoisomer.

Table 1.1. Results from $^1O_2$ reacting with the oxazolidinone substituted enecarbamate.

entry	substrate	conversion (%)	**MDB** (%e.e.)
1	(*Z*,4*R*,3'*R*)	49 ± 12	27 ± 4 (*R*)
2	(*Z*,4*S*,3'*S*)	47 ± 10	11 ± 2 (*S*)
3	(*E*,4*R*,3'*R*)	47 ± 3	55 ± 5 (*R*)
4	(*E*,4*S*,3'*S*)	50 ± 3	40 ± 8 (*S*)

The stereoselectivity of **1c** and **1d,** E-isomers, exhibited a temperature dependence, showing preference in reacting with the E4R3'S over the E4S3'R at lower temperatures in $^1O_2$ reactions. **1a** and **1b**, the Z-isomers, however, did not show this same temperature dependence in selectivity and only exhibited e.e. values of up to 27%. The following results in Table 1.2[14] show the temperature and solvent dependence for **1c** and **1d**.

Table 1.2. Results from reacting $^1O_2$ with E-4R,3'R/S and E-4S,3'R/S under varying conditions.

substrate	solvent	temp. (°C)	MDB (%e.e.)	conversion (%)
E4R3'*R/S*, **1c**	CD_3CN	50	64 (*S*)	23
		18	30 (*S*)	34
		-15	0	28
		-40	58 (*R*)	37
E4R3'*R/S*, **1c**	CD_3OD	50	70 (*R*)	30
		18	85 (*R*)	34
		-15	90 (*R*)	17
		-40	94 (*R*)	12
E4R3'*R/S*, **1c**	CD_2Cl_2	20	34 (*S*)	25
		-20	27 (*R*)	65
		-60	74 (*R*)	31
E4S3'*R/S*, **1d**	CD_2Cl_2	18	28 (*R*)	29
		-20	36 (*S*)	59
		-60	88 (*S*)	56
E4R3'*R/S*, **1c**	$CDCl_3$	50	8 (*S*)	5
		18	63 (*R*)	17
		-15	78 (*R*)	37
		-40	88 (*R*)	43

It is important to note the high selectivity (>90%) found when singlet oxygen reacts with **1c** in CD_3OD at cooler temperatures. This high selectivity is hard to obtain in photooxidation reactions.

Now that it is known which diastereomer singlet oxygen will preferentially react with (starting with a 50:50 racemic mixture), mechanistic hypotheses can be made to explain these preferences. One way to explore these hypotheses is to compare the $^1O_2$ reactions of the oxazolidinone substituted enecarbamates with those of other known and well studies enophile reagents.

1.5. Calculating Reaction Selectivity

At low reaction conversion, if the orientation of one diastereomer permits greater selectivity, then reacting $^1O_2$ with an epimeric mixture of the enecarbamates will yield an enantiomeric excess of one enantiomer of MDB over the other. The selectivity, either by analyzing the excess of product formed or by analyzing the unreacted substrates can be measured through Chiral GC or NMR, respectively. These values are determined by first taking a spectrum, (Figure 1.9 and 1.10 respectively), that demonstrates an equal concentration of the two disastereomers, then applying those integration values to Equation 1.1 below. The spectrum used can be either from the chiral GC of enantiomers or ^{1}H-NMR of the unreacted epimers.

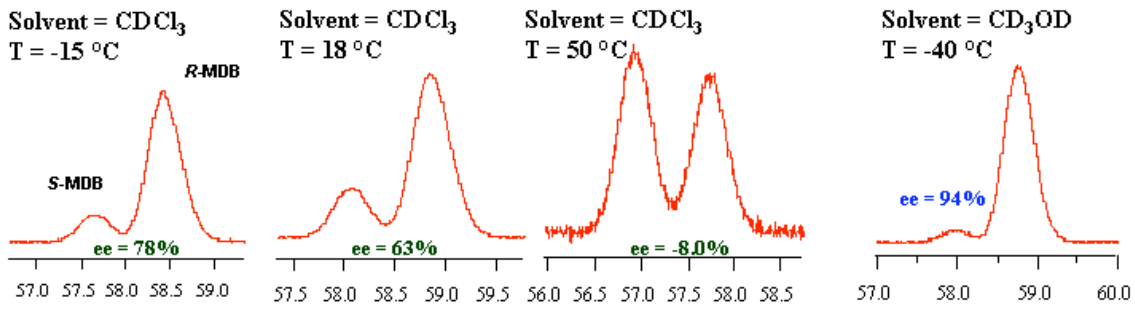

Figure 1.9. Chiral GC traces showing variability of selectivity with *E*-enecarbamates.

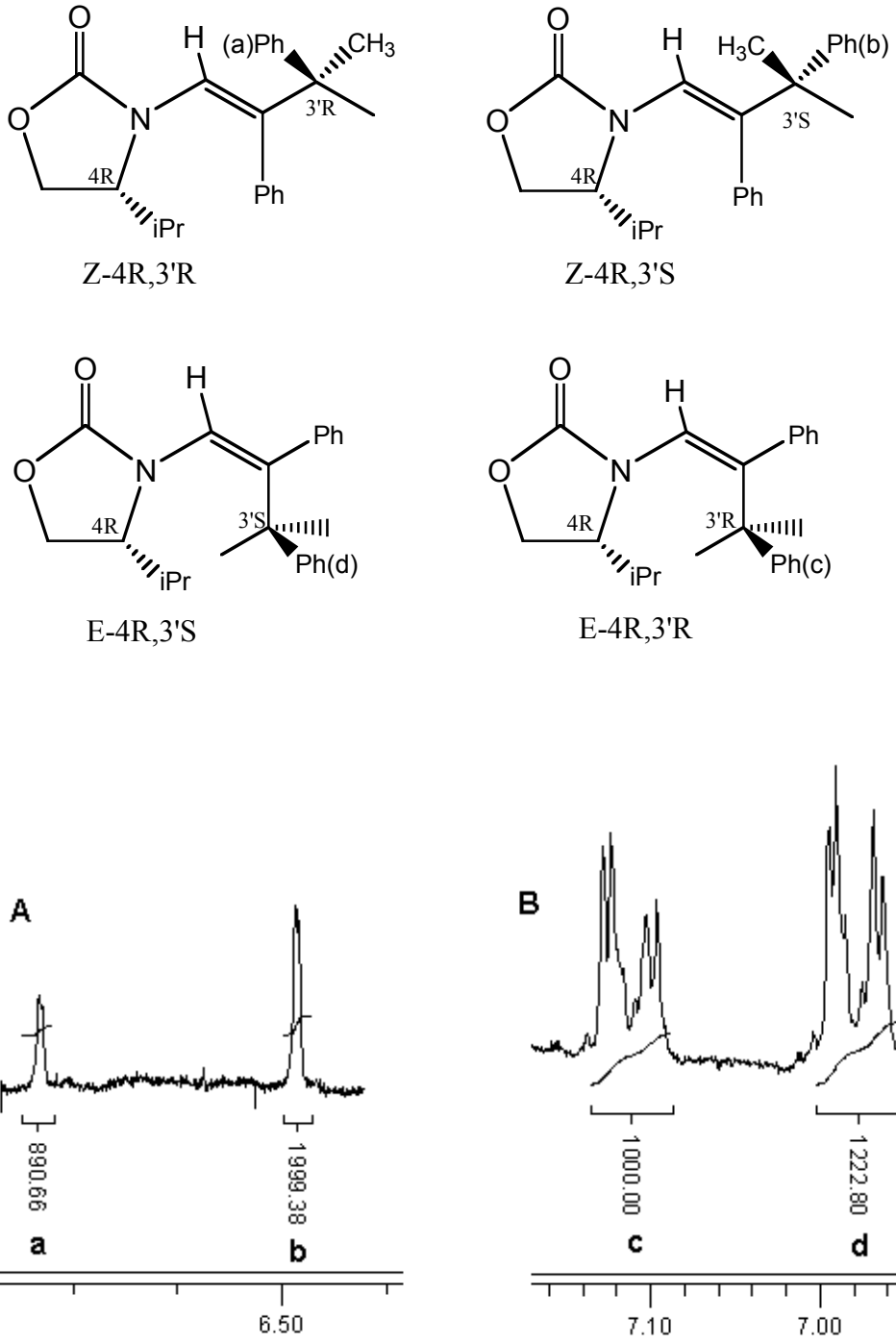

Figure 1.10. Representative ^{1}H NMR spectra showing resonances used to determine diastereotopic excesses of unreacted starting materials; **A**: *Z*-enecarbamates, **B**: *E*-enecarbamates. Specific hydrogens shown by spectra from the ortho protons on the phenyl group indicated above.

Equation 1.1. Calculation of enantiomeric or diastereotopic excess.

$$\%\text{e.e. or d.e.} = \frac{|A - B|}{|A + B|} \times 100$$

Where A = the sereoisomer in excess.

1.6. Ozonolysis Reactions.

Ozonolysis is the term used for the cleavage of alkenes by ozone. The mechanism for this reaction is vastly understood and accepted. Ozone attacks the double bonds in an orientation parallel to the bond. As shown in Scheme 1.3, the intermediate is an ozonide that is then cleaved to produce a carbonyl compound and a carbonyl oxide.[15] This forms an ozonide that, when reacted with sulfides, will cleave to form two carbonyls.[10]

Scheme 1.3. Ozonolysis

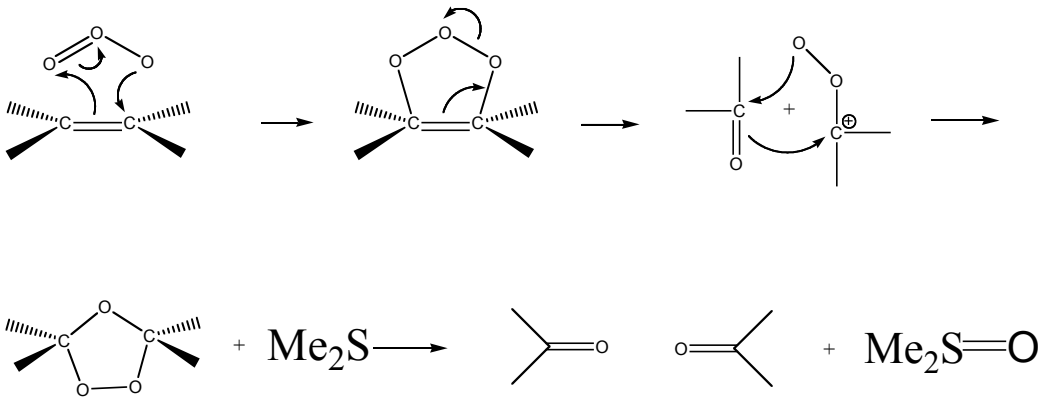

1.7. Reaction of Oxazolidinone Substituted Enecarbamates with Ozone.

Ozone (O_3) is a reactive ground-state species that is electrophilic in nature (similar to that of $^1O_2$). The reaction with enecarbamates **1a-d** and O_3 produces the same thermal decomposition products as does the reaction of enecarbamates with $^1O_2$ (Scheme 1.4 and 1.5).

Scheme1.4. $^1O_2$ and O_3 reacting with E-isomer.

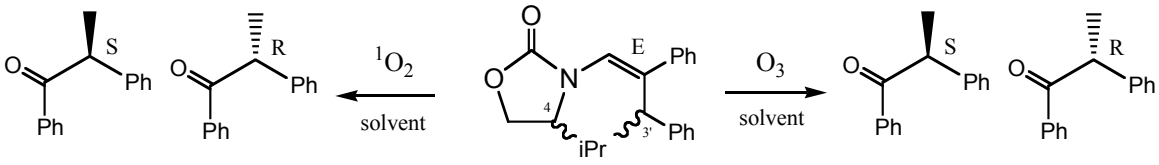

Scheme 1.5. $^1O_2$ and O_3 reacting with Z-isomer.

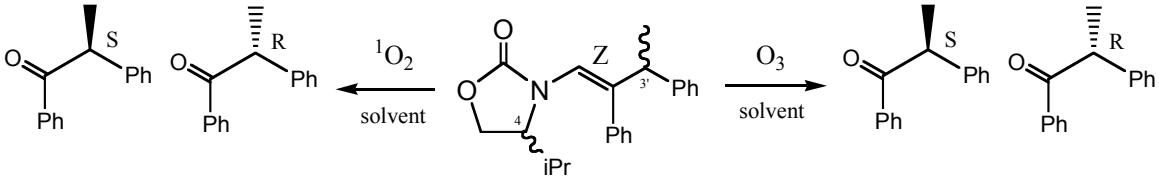

As shown in previous sections, ozone adds to double bonds via pericyclic a reaction. The main difference in the mechanism of these two reactions is the parallel addition of ozone to the double bond (Figure 1.11) versus the perpendicular addition of singlet oxygen (Figures 1.8.1 and 1.8.2).

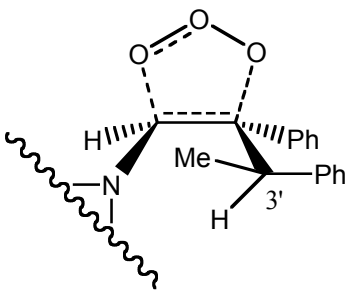

Figure 1.11. Ozone reaction with an oxazolidinone substituted enecarbamate.

Ozone was used to oxidize epimeric **1a-d** in CD_2Cl_2, $CDCl_3$, and CD_3OD at varying temperatures. Results showed only low selectivity compared to that found in the singlet oxygen reactions. Changing temperature did not significantly affect selectivity, while changes in reaction conversion had an inverse relationship to the e.e. values (i.e. when the conversion increased, selectivity decreased as in the reactions of **1b** at -70^{o}C in CD_2Cl_2). Changing the solvent also did not to affect e.e. values as dramatically as it did in the $^1O_2$ reactions (Table 1.3).[13]

Table 1.3.[16] Ozone Reaction of ozone with **1a-d** in varying solvents and temperatures.

Substrate	Solvent	Temp. (*C)	%e.e. MDB	Conversion
1c	CD_2Cl_2	20	22 (S)	6
		-15	24 (S)	15
		-45	16 (S)	18
		-70	18 (S)	27
1c	$CDCl_3$	20	18 (S)	12
		-15	20 (S)	17
		-70	29 (S)	25
1c	CD_3OD	20	4 (S)	4
		-15	2 (S)	6
		-45	0	4
		-70	4 (S)	5
1a	CD_2Cl_2	20	31 (R)	10
		-15	30 (R)	12
		-78	36 (R)	9
1b	CD_2Cl_2	20	33 (S)	6
		20	37 (S)	9
		-15	38 (S)	7
		-15	12 (S)	20
		-45	6 (S)	27
		-70	36 (S)	9
		-70	4 (S)	36
1b	$CDCl_3$	20	20 (S)	16
		-15	16 (S)	17
		-70	18 (S)	14
1b	CD_3OD	20	20 (S)	3
		-15	21 (S)	4
		-45	22 (S)	16
		-70	22 (S)	7

Data from these experiments mimicked the singlet oxygen results to prove that the enhanced MDB enantiomer depends on the configuration of the C-4 position of the oxazolidinone ring. This can be seen in the selectivity of ozone reacting with **1a** compared to **1b**. Changing the stereochemistry on the chiral auxiliary from 4R to 4S changed the sense of the ee from S-MBD to R-MBD. In general, when reacting with O_3, the Z-isomer displays comparable or higher stereoselectivity than the corresponding E-isomer. This is in contrast to the observed trend $^1O_2$, for which the E-isomer exhibits a

very high stereoselectivity (e.e.>97% in CD_3OD at -70°C) compared to the Z-isomer. This discrepancy lead us to explore the issue of chemical quenching of singlet oxygen driving selectivity versus physical quenching. In other words, is the isopropyl group at C-4 influencind the attack of $^1O_2$ via sterics, vibrational deactivation, or both? At this point it was also important to test the role of the substituents at C-3' in determining stereoselectivity (i.e. how these groups may inhibit $^1O_2$ from attacking the double bond through deactivation or steric blocking). Physical quenching (over steric hindrance) has not been previously cited as a predominate factor in driving stereoselectivity. Were this to be the proven, it could influence how chemists discuss singlet oxygen reactivity in future (and past) studies.

1.8. Physical Versus Chemical $^1O_2$ Quenching.

Previously determined time-resolved $^1O_2$ quenching studies showed that total $^1O_2$ quenching by **1a-d** is mostly due to physical, rather than chemical quenching.[14] This suggests that the selectivity seen in these reactions may relate to the excited state nature of $^1O_2$, since it may be vibrationally deactivated upon encountering C-H bonds. In other words, the origin of stereoselectivity for the reactions of **1a-d** with $^1O_2$ may *not* be purely due to sterics (Figure 1.12).

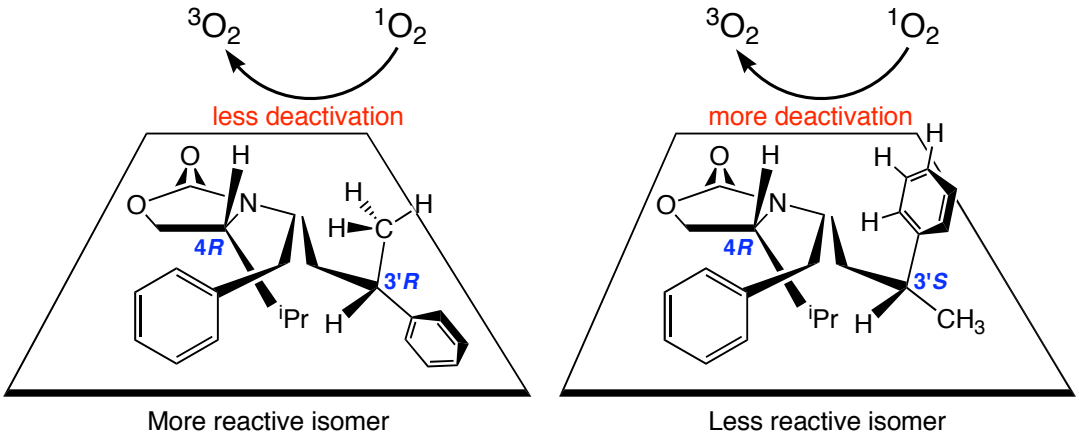

Figure 1.12.Illustration showing how C-H vibrational deactivation, rather than sterics, may lead to stereodifferentiation of **1a** by $^1O_2$.

1.9. N-phenyl-1,2,4-triazoline-3,5-dione (PTAD)

To determine whether vibrational deactivation of $^1O_2$ plays a role in the stereoselectivites observed with the enecarbamates, more evidence is needed. We sought a bulkier reagent that would react similarly to $^1O_2$, but that would not be subject to vibrational deactivation. A molecule called N-phenyl-1,2,4-triazoline-3,5-dione (PTAD) (Figure 1.13) possesses these characteristics and proved to reveal a great deal about what is going on with singlet oxygen.

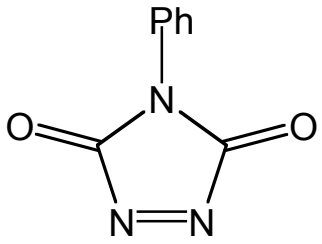

Figure 1.13. N-phenyl-1,2,4-triazoline-3,5-dione (PTAD).

It has been shown, that PTAD is a reactive enophile that has been shown to yield products analagous to those produced when $^1O_2$ is reacted with alkenes. In fact, the mechanistic pathways that both PTAD and $^1O_2$ are thought to undergo, are quite similar. This is made evident when comparing Figure 1.14 below to Figure 1.9.1 above.

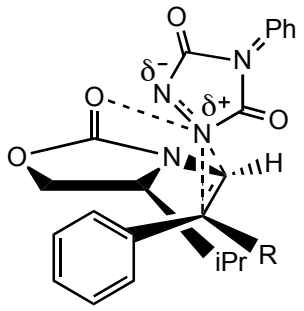

Figure 1.14. PTAD transition state upon reaction with alkenes.

As the figure above shows, the addition of PTAD to the double bond is perpendicular, just like that seen in the addition of singlet oxygen to the double bond. The major differences are that 1) PTAD is a much larger enophile and therefore will experience more selectivity than $^1O_2$ if sterics is the deciding factor and 2) PTAD reacts in its ground state and is not subject to deactivation. The stereochemistry at the C-3' position is of interest because it contains the substituents (CH_3 versus Ph) that have the potential to sterically or deactivationally block the singlet oxygen from reacting with the double bond. Reacting PTAD with **1a-d** under similar conditions as that found in Table 1.2 will help determine whether it is sterics or vibrational deactivation that drives selectivity of the singlet oxygen reactions, bringing clarity to the importance of the C-3' position. If PTAD shows equal or stronger selectivity than was found in the $^1O_2$ reactions

with **1a-d**, steric hindrance at the C-3' center will be the likely explanation for this selectivity. If PTAD shows less selectivity when reacting with **1a-d** than did singlet oxygen, the conclusion can be made that sterics at the C-3' chiral center *does not* drive the selectivity, but rather vibrational deactivation would.

Reactions were carried out in $CDCl_3$ with quantitative amounts of PTAD and **1a-d** at varying temperatures (24, 7.0 and -20^{o}C). Reaction conversions were kept low by limiting the amount of PTAD to less than one equivalent and monitoring the reactions by following the rate of disappearance of the characteristic red color. Diastereotopic excess was determined using ^{1}H-NMR as illustrated in Section 1.6. At low conversion ($\leq 20\%$) stereoselectivity is mostly temperature independent and much less than that seen with $^{1}O_2$. These results and their implications are presented herein.

Chapter 2: Experimental

2.1. Materials.

E-enecarbamates were provided by J. Sivaguru (Columbia Univ.). All Solvents and Reagents were used as recovered from Aldrich Chemical Company. Z-enecarbamates were synthesized from methyl phenylacetate as described below.

2.2. Enecarbamate Synthesis.

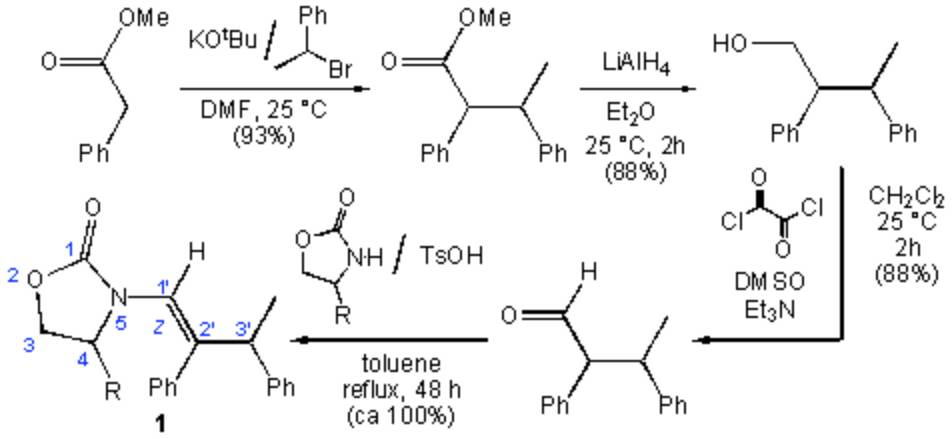

Figure 2.2. Synthesis of **1a** and **b** from methyl 2-phenylacetate.[10]

2.2.1. Methyl-β-Methyl-α-Phenylbutyrate.

A 4.8604g sample of potassium t-butoxide were placed in 30ml of dry DMF at 0°C. Upon addition, the t-butoxide did not readily dissolve. A stirring rod was used to break up the solid in order to speed the dissolving process. About 4.8ml of methyl phenylacetate was added, turning the solution red. After three minutes of stirring, 4.5ml of 1-bromoethyl benzene were added. The reaction was left to warm to room temperature followed by stirring for an hour. After one hour, 40ml of water were added to the solution, terminating the reaction. This solution was left to stir over night.

The product, methyl-β-methyl-α-phenylbutyrate, had solidified in the solution. After 40ml CH_2Cl_2 was added to solution, ultrasonication was used to dissolve the

clumped white precipitate. The aqueous layer and organic layer with product were separated and the aqueous layer was extracted again with 40ml CH_2Cl_2. The organic layers were combined and washed two times with 40ml of a saturated aqueous solution of NH_4Cl. The solution was dried over $MgSO_4$ and the solution evaporated off, however, not all the solvent was removed. To remove the rest of the solvent the solution was filtered through a filter funnel using a small amount of water as the wash. The final yield of pure product was 6.6421g (81.0% yield) of the methyl-β-methyl-α-phenylbutyrate.

2.2.2. 2,3-Diphenyl-1-butanol.

To make the next intermediate in the synthesis, 2,3-Diphenyl-1-butanol, the 6.6421g of methyl-β-methyl-α-phenylbutyrate was dissolved in about 40ml of ethyl ether and slowly added to 30ml of 1M $LiAlH_4$ in a argon atmosphere. The reaction was monitored by TLC while stirring. The reaction was terminated by the slow addition of water. This was done only after precautions were taken to make sure there was not a highly active amount of $LiAlH_4$ left in solution. A solid had formed, these were the byproducts $Al(OH)_3$ and LiOH. The contents of the flask were poured over a large filter funnel. A large amount of the white byproduct was removed. The filter was washed with 100ml of CH_2Cl_2. The organic layer was washed with (2 x 50ml) NH_4Cl_4. The organic layer, which still contained a large amount of NH_4Cl_4 and byproduct, was dried over $MgSO_4$ causing the salts to precipitate allowing for separation of the organic layer with product from the byproducts. 2.4974g of pure product were obtained, equaling a 43% yield.

2.2.3. 2,3-Diphenylbutyraldhyde.

The 2,3-Diphenyl-1-butanol was then converted to 2,3-Diphenylbutyraldhyde via the Swern Oxidation. A 1.5ml sample of 1.5ml oxalylchloride was added to a solution of 55ml CH_2Cl_2 and was cooled to -78^oC . To this, 2.4ml DMSO in 9ml CH_2Cl_2 was added. This solution was left to stir for ten minutes before the 2.4974g of 2,3-Diphenyl-1-butanol was added. After another 15 minutes, pure Et_3N was added. The solution was left to stir for one hour. To terminate the reaction 30 ml of H_2O was added. The phases were then separated and the aqueous layer was extracted with 2 x 50ml CH_2Cl_2. The organic layers were combined and washed with 100ml H_2O. The organic layer was dried over $MgSO_4$. The solvent was evaporated off, leaving the crude 2,3-diphenylbutyraldhyde product.

The product was purified by silica gel flash chromatography using a petroleum ether/ ethyl acetate (4:1) mobile phase. The column was monitored with TLC. A 1.8324g sample of the pure 2,3-diphenylbutyraldhyde was obtained. ^{1}H-NMR was used to verify the product was obtained.

2.2.4. 3-[(1Z)-2,3(S,R)-diphenylbut-1-enyl]-4(S)-isopropyloxazolidin-2-one (1b).

In order to make the 3-[(1Z)-2,3(S,R)-diphenylbut-1-enyl]-4(S)-isopropyloxazolidin-2-one, 0.5036 g of 2,3-diphenylbutyraldhyde and 0.2536g of (S)-(-)-4-isopropyl-2-oxazolidinone were mixed in a 25ml round bottom flask half full of toluene. About 0.0031g (a catalytic amount) of p-toluenesulfonic acid was added. A calcium carbonate column was placed above the flask to trap the water produced on the reaction. The reaction was run at about 60^oC under reflux and left for 12 hours. It was

important to make sure the solvent did not evaporate off during this process, which would cause the reactants to oxidize.

After the reaction was terminated, the product was partitioned with 25ml NH_4Cl solution and the organic layer was collected. This was then dried over $MgSO_4$. Purification was achieved with silica gel flash chromatography. Petroleum ether: ethyl acetate (4:1) was first used as the mobile phase, this did not lead to a successful separation so a second column was run using CH_2Cl_2. The column was monitored with TLC and GC/MS to make the initial verification that the product was obtained. The product came out in the later fractions on the column. After evaporation of solvent, 0.3668g of the pure product were obtained and dissolved in 10ml of chloroform-d to make a 0.1093M solution of the product. ^{1}H-NMR was used to verify the desired product was obtained.

2.2.5. 3-[(1Z)-2,3(S,R)-diphenylbut-1-enyl]-4(R)-isopropyloxazolidin-2-one (1a).

This same process (section 2.2.4) was repeated using the (S)-(-)-4-isopropyl-2-oxazolidinone to produce 3-[(1Z)-2,3(S,R)-diphenylbut-1-enyl]-4(R)-isopropyloxazolidin-2-one. A 0.5108g sample of the starting aldehyde was used and 0.1328g of pure product was obtained. This was then dissolved in 3.5ml of Chloroform-d to obtain a 0.1131M solution of the 3-[(1Z)-2,3(S,R)-diphenylbut-1-enyl]-4(R)-isopropyloxazolidin-2-one. ^{1}H-NMR was used to verify the product was obtained.

2.3. Reaction of Enecarbamates with PTAD.

In order to get a small conversion in this reaction 130µl of the respective enecarbamate solution (diastereomer 4R or 4S) was put into an NMR tube. A small

recorded amount of the PTAD (varying between 0.200 to 0.500mg for each sample) dissolved in chloroform-d was added to the NMR tube where the reaction would be carried out. Once the solution was no longer red, the reaction had terminated. A ^{1}H-NMR spectra was obtained for each reaction set after it had terminated. Conversion and diastereometric excess was calculated and recorded for each reaction set.

Three reactions for both the Z-R and S Enecarbamate (**1a** and **b**) were run at 24^{o}C, 7.0^{o}C and -20^{o}C. NMR was taken for each of the reactions. This same procedure was used with the E-enecarbamates (**1c** and **d**). Calculations were done to make sure the correct mole ratios were used to achieve desirable reaction conversions. One again about 0.200 to 0.500mg of PTAD was used for each reaction.

2.4. Instrumental Materials.

^{1}H-NMR spectra were obtained on a Bruker AC360 spectrometer using NTNMR software version 1.3 and processed with Mestre-C 4.1.1.0. All NMR were dissolved in $CDCl_3$ without TMS, due to interferences it would have on the reactions. GC/MS data were obtained with a Varian CP-3800 gas chromatograpy which uses a CP-Sil 8 column, Saturn 2200 mass spectrometer, and CP-8400 autosampler.

Chapter 3: Results.

NMR analysis of PTAD reactions with **1a-d** are summarized in Tables 3.1-3.8. Figures 3.1 through 3.4 show partial ^{1}H-NMR spectra of the resonances of interest for **1a-d** before the addition of PTAD. Figures 3.5.1- 3.8.6 show spectra and integrations of diastereotopic hydrogen peaks for each PTAD reaction run with **1a-d** at the varying temperatures.

Table 3.1 summarizes the results for the reactions of **1a** and PTAD. Three trials were taken at the three different temperatures, 24, 7.0 and –20^{o}C demonstrate any trends that might exist with varying temperature. Comparative peak integrations of diastereotopic hydrogens are displayed along with d.e. values calculated from those integrations. The spectra for **1a-d** prior to reaction are displayed in Figures 3.1, 3.3, 3.5-3.8. Figures 3.3 and 3.5 show that the initial 5d.e. for 1a determined from the hydrogens of interest is about 7% (3'S). This skews the %d.e. determinations slightly for the **1a** epimers and explains why %d.e. results for 1a are slightly higher in magnitude than for **1b**. The peaks of interest are displayed in Figures 3.5.1 – 3.5.9 and represented in Table 3.1 as well. The exact percent conversion expressed throughout each table was determined though knowledge of the amount of PTAD used in each reaction and the assumption that all the PTAD had reacted (the solution becomes colorless when PTAD is completely consumed). As temperature decreases, results show a slight increase in selectivity. This increase in selectivity, however, is within the standard deviation. Z-4R,3'S is the species in diastereotopic excess (the less reactive epimer) for each of these trials and temperatures.

Table 3.1. Reactions of **1a** with PTAD in $CDCl_3$ at varying temperatures.

Temp (^oCt)	Integration (1)[a]	Integration (2)[b]	d.e. value	%conversion	average	standard dev
24	1000	1193	8.78	16.4	10.2	1.2
24	1000	1245	10.9	17.6		
24	1000	1247	11.0	22.6		
7	1000	1216	9.76	12.3	12.5	3.2
7	1000	1267	11.8	12.9		
7	1000	1384	16.1	13.2		
-20	1000	1303	13.2	15.8	13.8	3.7
-20	1000	1234	10.5	18.0		
-20	1000	1434	17.8	22.5		

[a] integration for peak representing Z4R3'R
[b] integration for peak representing Z4R3'S

Table 3.2 shows this same information shared above except for the **1b** PTAD reactions. These d.e. values are taken from the comparative integration values shown in the table and in figures 3.6.1 – 3.6.9. Z4S3'R is the species in diastereotopic excess (the less reactive epimer) for all of these trials except trial 3 at 24^{o}C.

Table 3.2. Reactions of **1b** with PTAD in $CDCl_3$ at varying temperatures.

Temp (^oC)	Integration (1)[a]	Integration (2)[b]	d.e. value	%conversion	average	standard dev
24	1000	1006	0.299	14.1	0.333	4.0
24	1000	1092	4.37	15.2		
24	1000	929.1	-3.68	19.4		
7	1000	1058	2.80	16.6	3.72	1.1
7	1000	1103	4.89	17.8		
7	1000	1072	3.47	19.5		
-20	1000	1093	4.43	17.4	4.36	0.4
-20	1000	1098	4.67	17.7		
-20	1000	1083	3.96	18.4		

[a] integration for peak representing Z4S3'S
[b] integration for peak representing Z4S3'R

Tables 3.3 and 3.4 show the results for the reactions of the E-enecarbamates, **1c** and **1d**, respectively, with PTAD in $CDCl_3$ at various temperatures. Diastereoselectivities are determined as before using integration values from the ^{1}H-NMR spectra shown in figures 3.7.1 through 3.8.6. As seen with $^1O_2$,[13] selectivity is higher with the E-isomers than with the Z-isomers. Data from the reaction of PTAD with **1d** at -20°C are unavailable due to a shortage of the starting material. However, at this point, the data from each reaction seem consistent enough to preclude the need for this data. In fact. the results in these trials are consistent with previously reported trends in selectivity for reactions of chiral enecarbamates where the reactions of the optical antipodes at C-4 (e.g. E4R3'R/S versus E4S3'R/S) give similar selectivity, but opposite in sense. That is, the E4R3'R isomer is more reactive with PTAD for the **1c** epimeric pair, while the E4S3'S isomer is more reactive when the **1d** epimeric pair is reacted with PTAD.

Table 3.3. Reactions of **1c** with PTAD in $CDCl_3$ at varying temperatures.

Temp (*C)	Integration (1)	Integraion (2)	d.e. value	%convertion	average	standar dev
24	1000	1309	13.4	16.4	14.3	1.5
24	1000	1382	16.0	16.8		
24	1000	1310	13.4	17.8		
7	1000	1248	11.0	20.1	8.00	3.1
7	1000	1178	8.2	20.6		
7	1000	1103	4.9	20.7		
-20	1000	1252	11.2	14.5	11.2	0.8
-20	1000	1233	10.4	16.9		
-20	1000	1274	12.0	17.4		

[a] integration for peak representing E4R3'R
[b] integration for peak representing E4R3'S

Table 3.4. Reactions of **1d** with PTAD in $CDCl_3$ at varying temperatures.

Temp (^oC)	Integration (1)[a]	Integration (2)[b]	d.e. value	%conversion	average	standard dev
24	1000	1269	11.9	16.2	12.6	0.7
24	1000	1296	12.9	17.7		
24	1000	1301	13.1	22.1		
7	1000	1209	9.46	17.2	10.5	0.9
7	1000	1254	11.3	22.8		
7	1000	1240	10.7	24.0		

[a] integration for peak representing E4S3'S
[b] integration for peak representing E4S3'R

Table 3.5. Averages values for reactions of **1a-d** with PTAD

Enecarbamate	Temp. (^oC)	average d.e.	standard dev.
E4R3'R,S	24	14.3	1.5
	7	8.00	3.1
E4S3'R,S	24	12.6	0.7
	7	10.5	0.9
Z4R3'R,S	24	10.2	1.2
	7	12.5	3.2
	-20	13.8	3.7
Z4S3'R,S	24	0.333	4.0
	7	3.72	1.1
	-20	4.36	0.4

Tables 3.6 and 3.7 show the affects on varying PTAD reaction conversion with **1c** and **d** respectively on the d.e. values. The data displaying the interaction of PTAD with **1c** and **d**, respectively, shows that conversion does not significantly affect the d.e. values. The d.e. values were calculated from the respective comparative integrations shown in Tables 3.6 and 3.7. The spectra used to obtain these integral values are displayed in Figures 3.13.1 through 3.15.3.

Table 3.6. Reaction of **1c** with PTAD in $CDCl_3$ at varying reaction conversions.

Conversion	Integration (1)[a]	Integration (2)[b]	d.e.
10%	1000	1599	23.0
20%	1000	1758	27.5
40%	1000	1552	21.6

[a] integration for peak representing E4R3'R
[b] integration for peak representing E4R3'S

Table 3.7. Reaction of **1d** with PTAD in $CDCl_3$ at varying reaction conversions.

Conversion	Integration (1)[a]	Integration (2)[b]	d.e.
10%	1000	1223	10.0
20%	1000	1177	8.1
40%	1000	1191	8.7

[a] integration for peak representing E4S3'S
[b] integration for peak representing E4S3'R

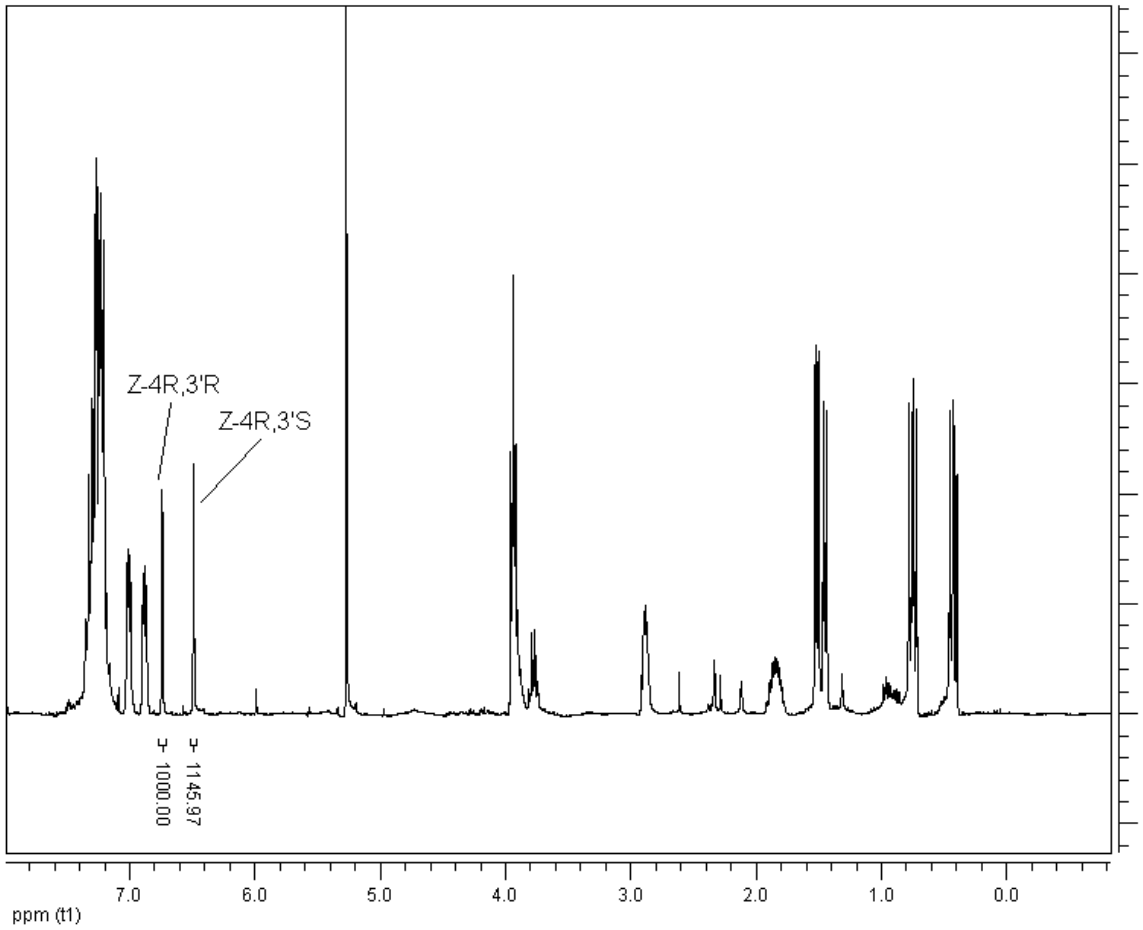

Figure 3.1. Full ^{1}H-NMR spectrum of Z-4R,3'R/S before reaction. The peak at 5.32 ppm represents dichloromethane.

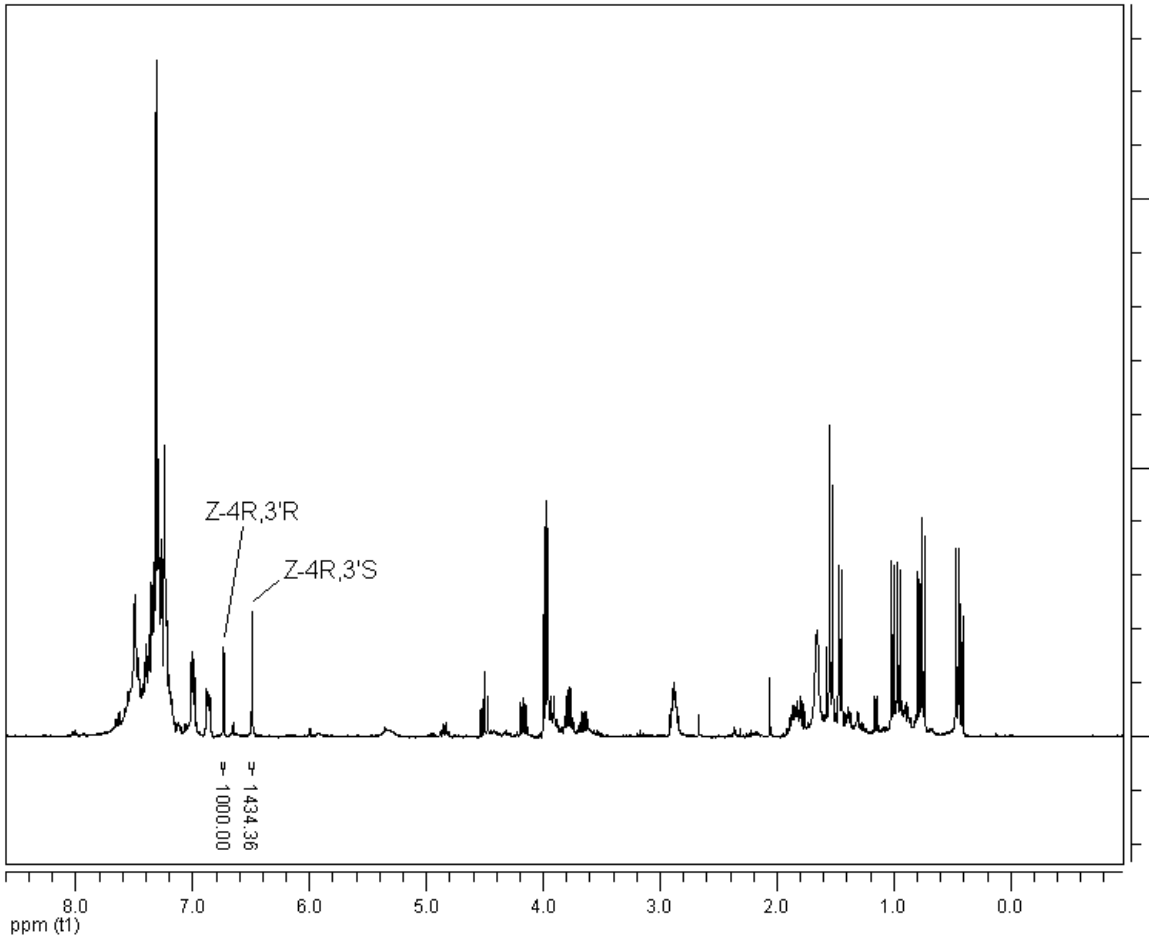

Figure 3.2. Representative full ^{1}H-NMR spectrum of Z-4R,3'R/S (**1a**) and PTAD after reaction.

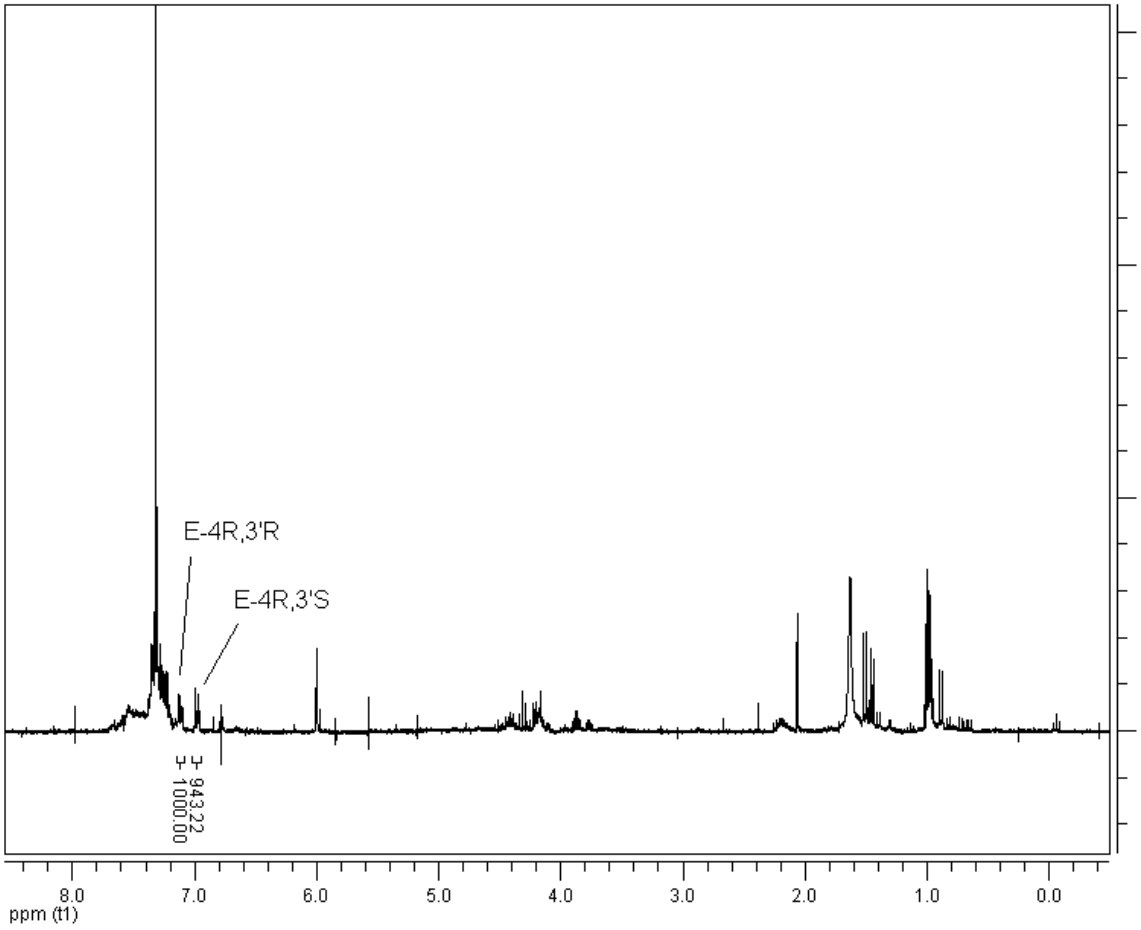

Figure 3.3. Full ^{1}H-NMR spectrum of E-4R,3'R/S (**1c**) before reaction.

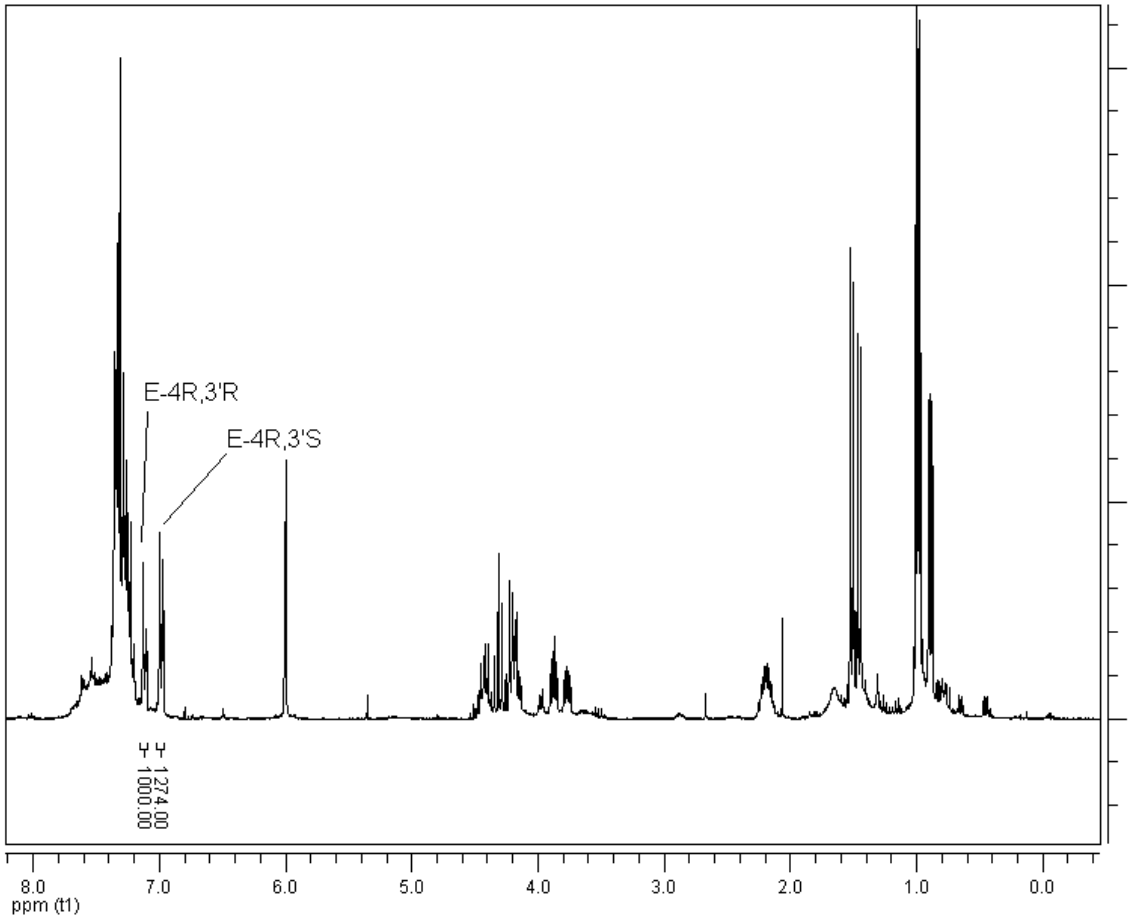

Figure 3.4. Representative full ^{1}H-NMR spectrum of E-4R,3'R/S (**1c**) and PTAD after reaction.

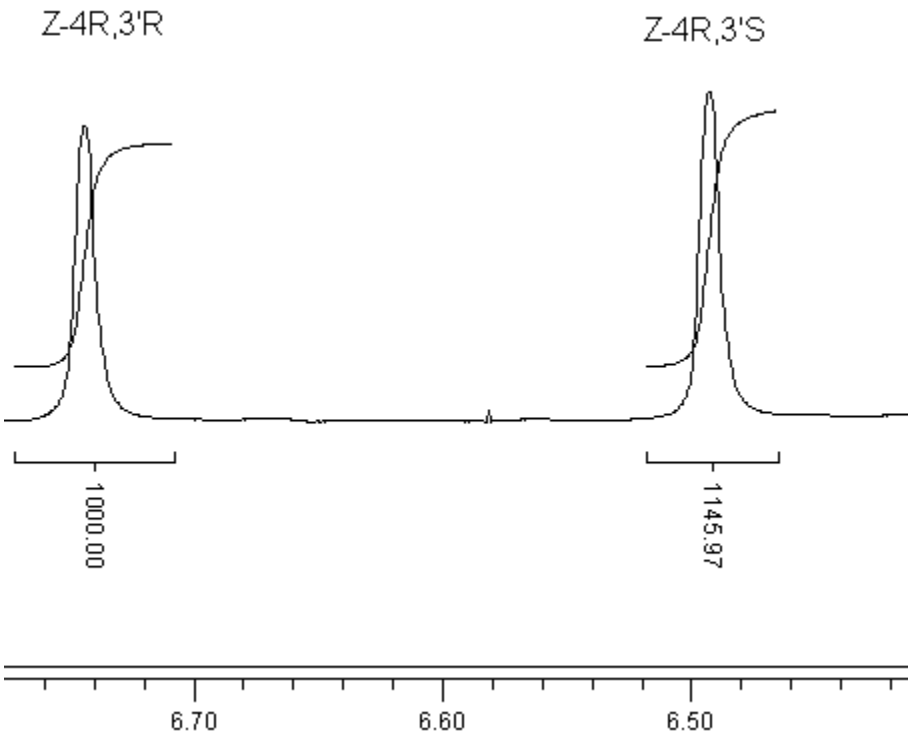

Figure 3.5. [1]H-NMR of **1a** before reacting with PTAD. Integration of vinyl proton signals shows a ca. 1:1 mixture.

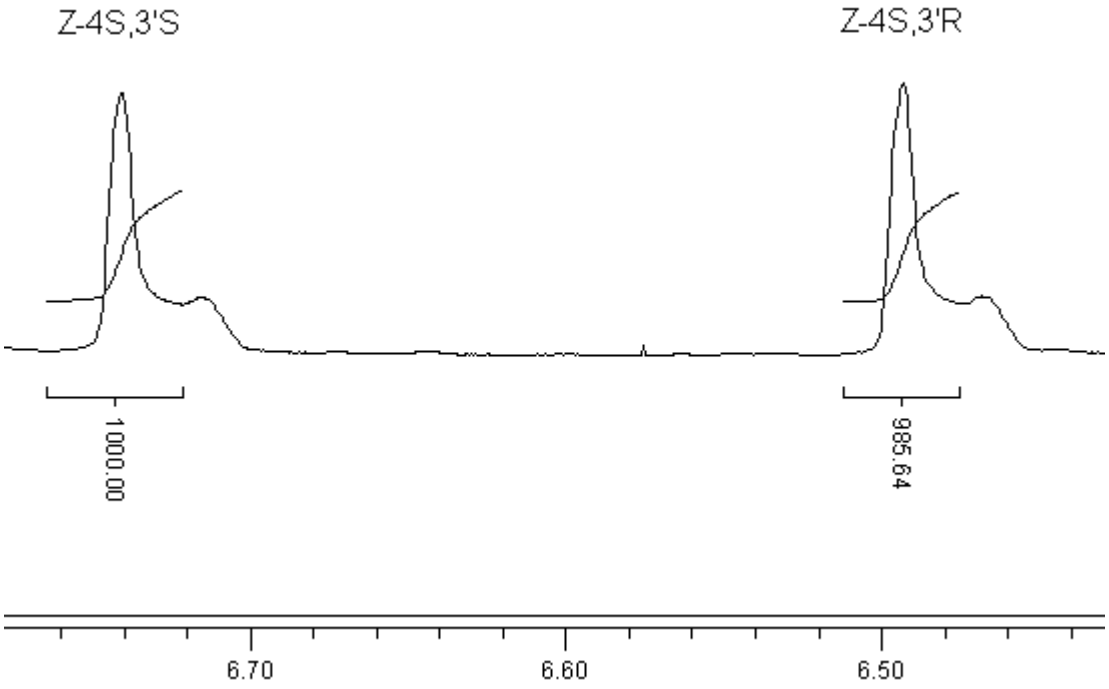

Figure 3.6. [1]H-NMR of **1b** before reacting with PTAD. Integration of vinyl proton signals shows a ca. 1:1 mixture.

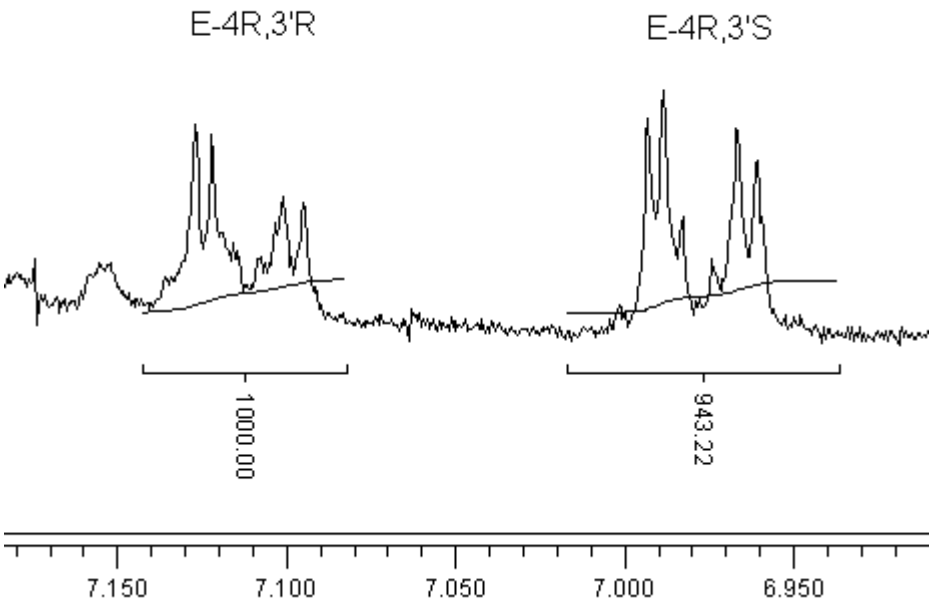

Figure 3.7. ^{1}H-NMR of **1c** before reacting with PTAD. Integration of vinyl proton signals shows a ca. 1:1 mixture.

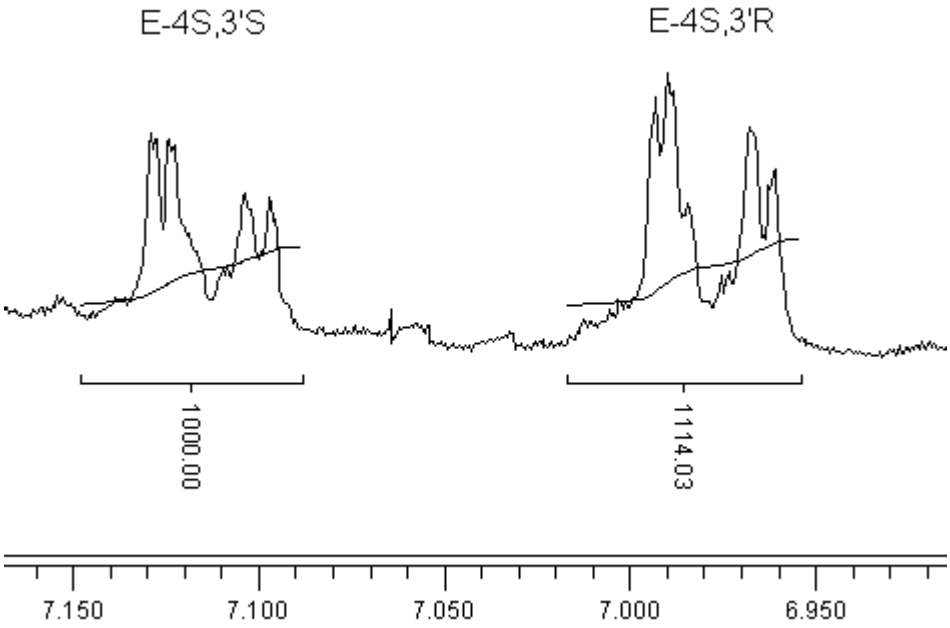

Figure 3.8. ^{1}H-NMR of **1d** before reacting with PTAD. Integration of vinyl proton signals shows a ca. 1:1 mixture.

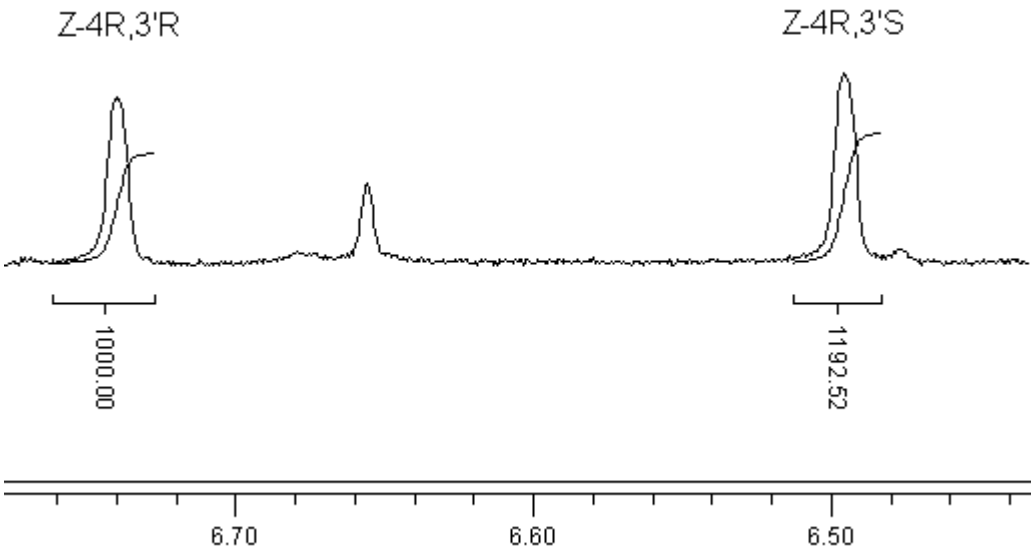

Figure 3.9.1. Trial 1, reaction of **1a** with PTAD (16.4% conversion at 24°C in $CDCl_3$).

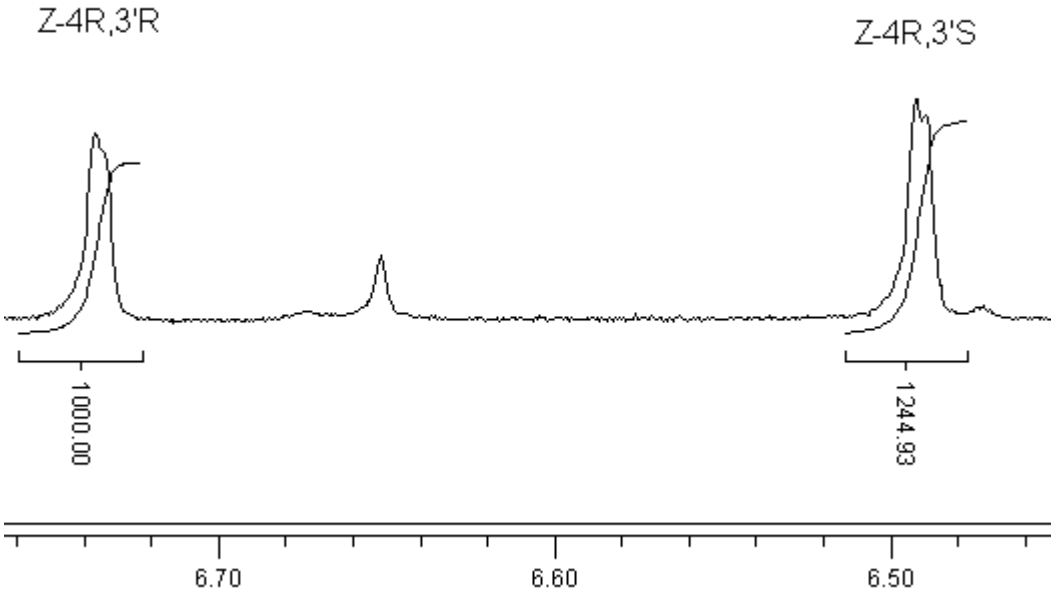

Figure 3.9.2. Trial 2, reaction of **1a** with PTAD (17.6% conversion at 24°C in $CDCl_3$).

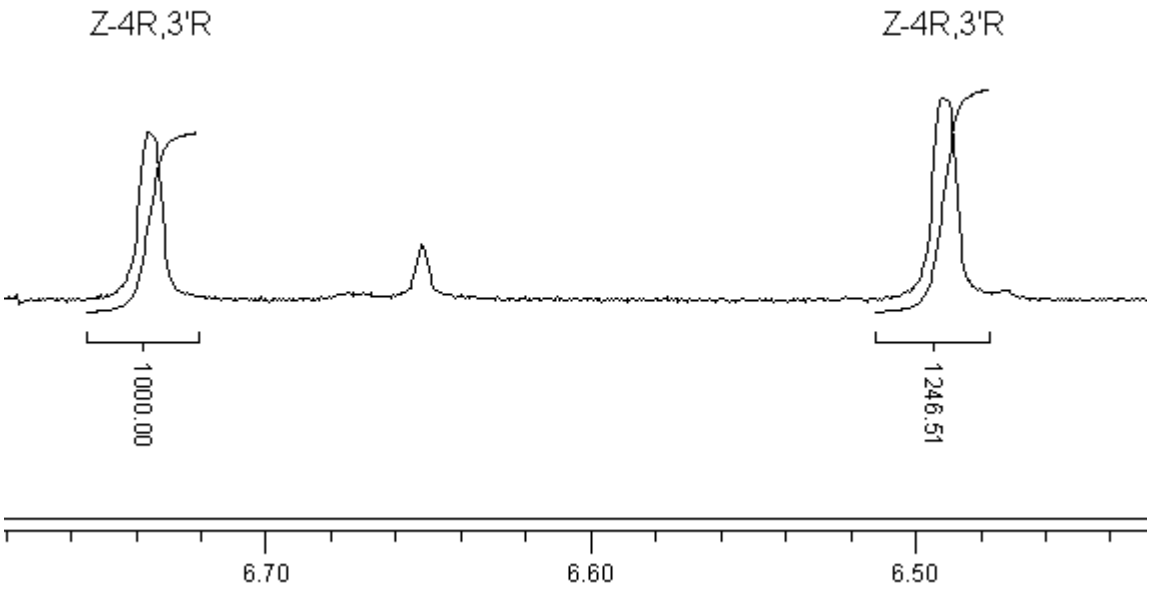

Figure 3.9.3. Trial 3, reaction of **1a** with PTAD (22.6% conversion at 24°C in $CDCl_3$).

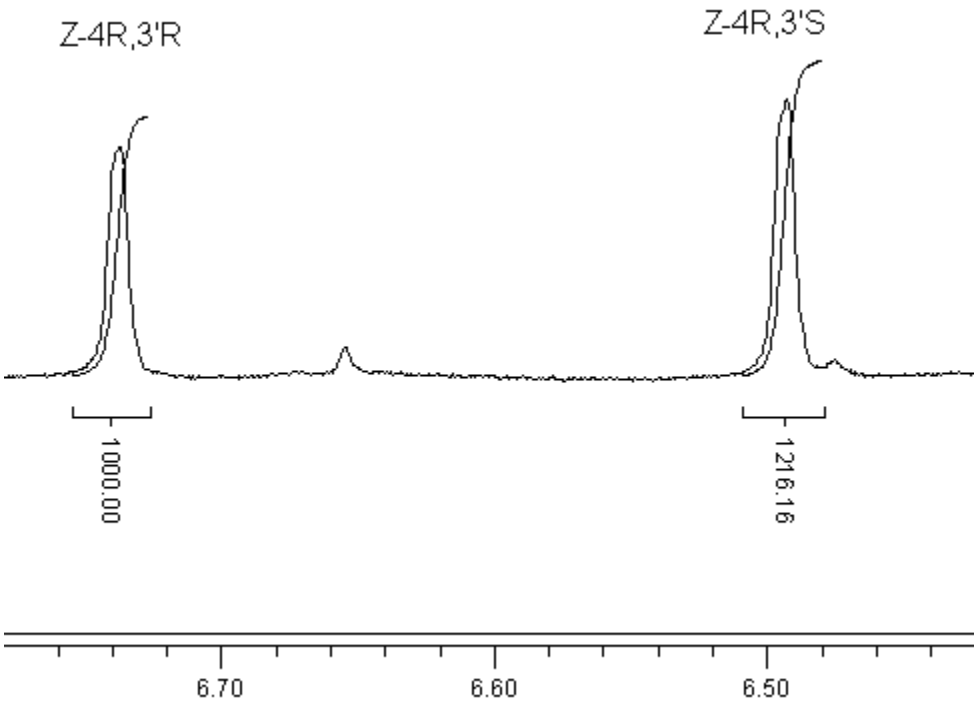

Figure 3.9.4. Trial 1, reaction of **1a** with PTAD (12.3% conversion at 7.0°C in $CDCl_3$).

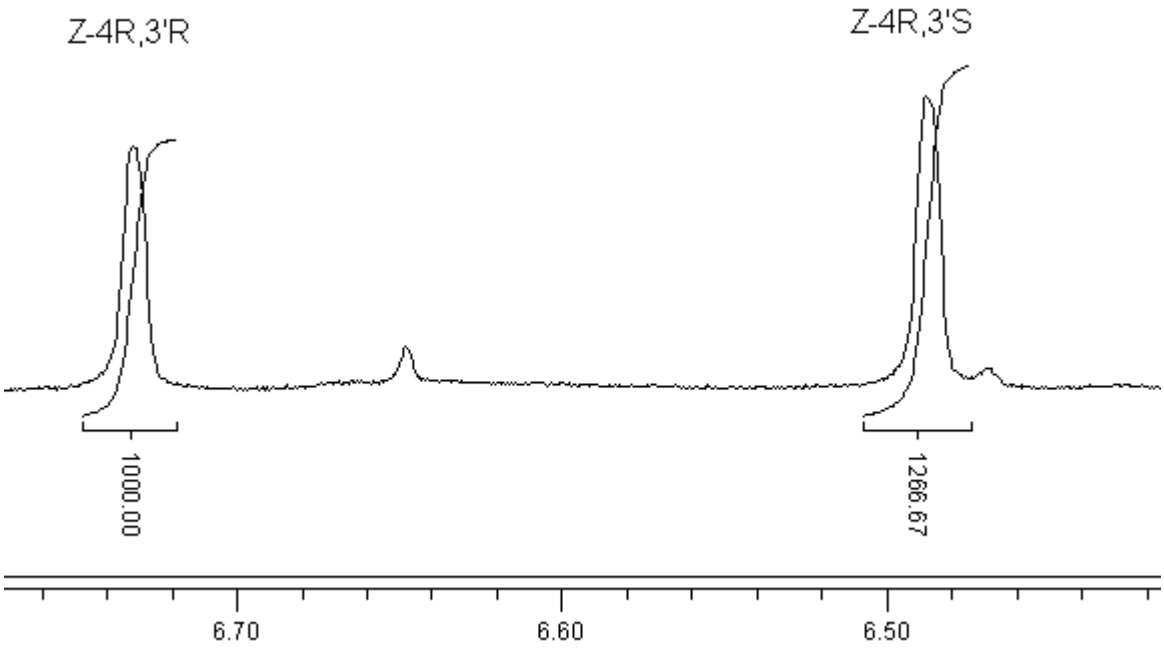

Figure 3.9.5. Trial 2, reaction of **1a** with PTAD (12.9% conversion at 7.0°C in $CDCl_3$).

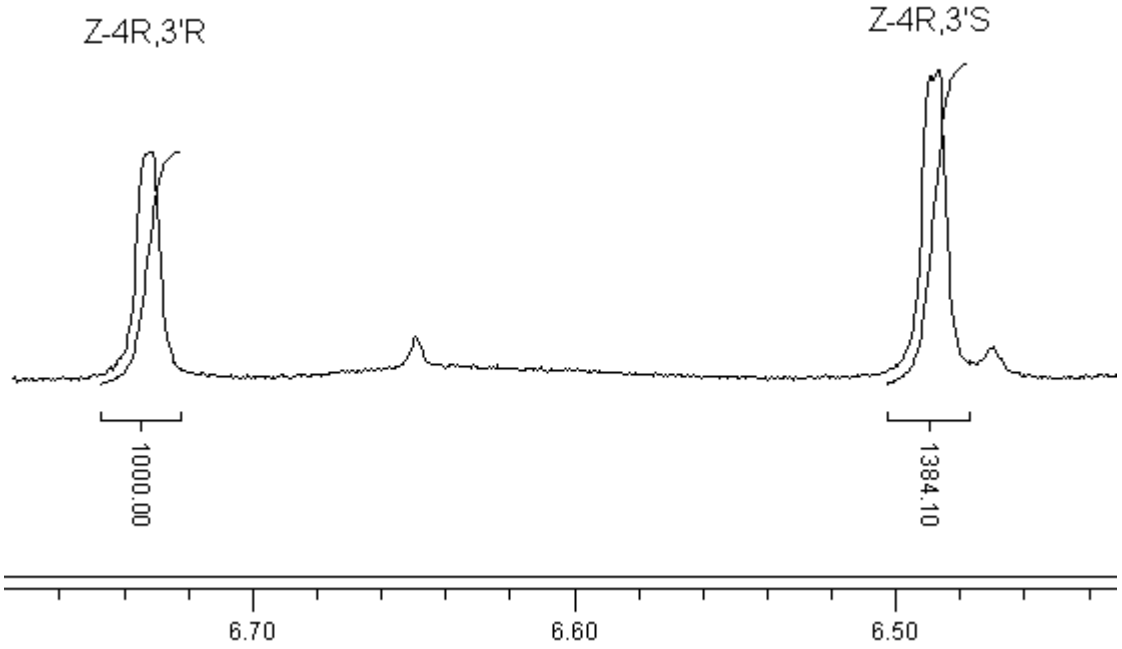

Figure 3.9.6. Trial 3, reaction of **1a** with PTAD (13.2% conversion at 7.0°C in $CDCl_3$).

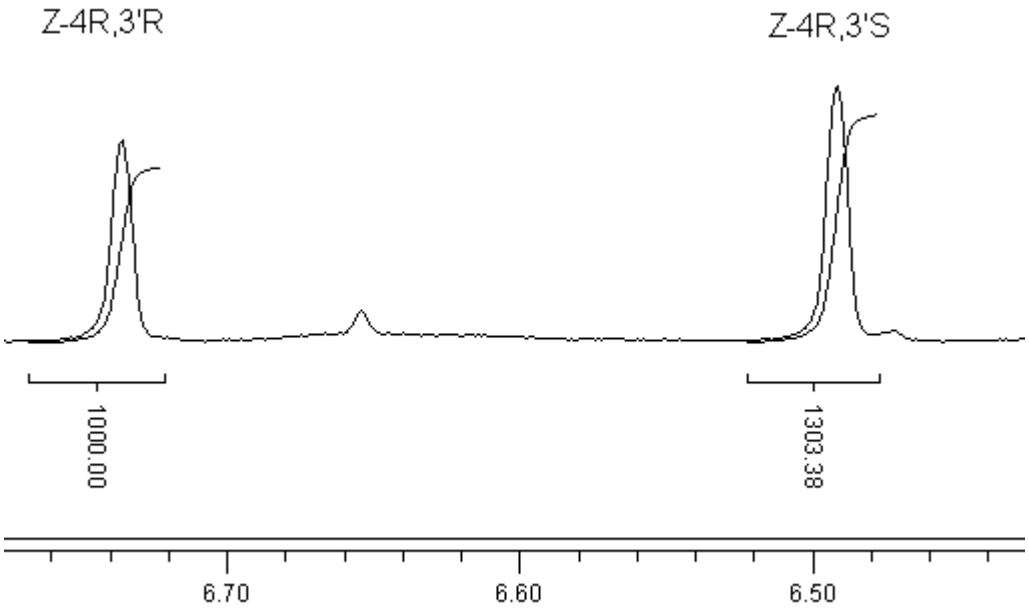

Figure 3.9.7. Trial 1, reaction of **1a** with PTAD (15.8% conversion at -20°C in $CDCl_3$).

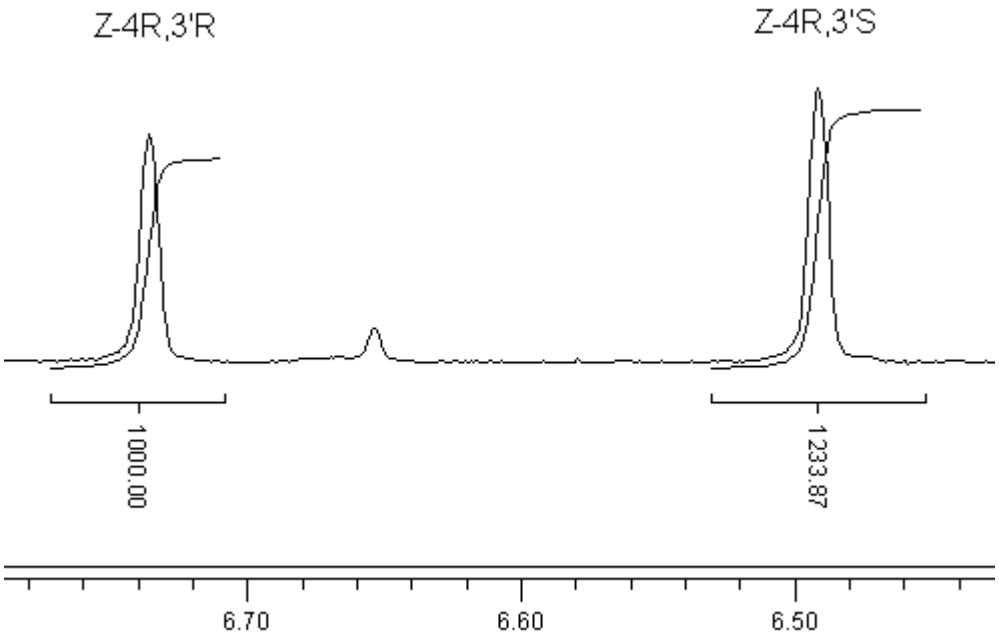

Figure 3.9.8. Trial 2, reaction of **1a** with PTAD (18.0% conversion at -20°C in $CDCl_3$).

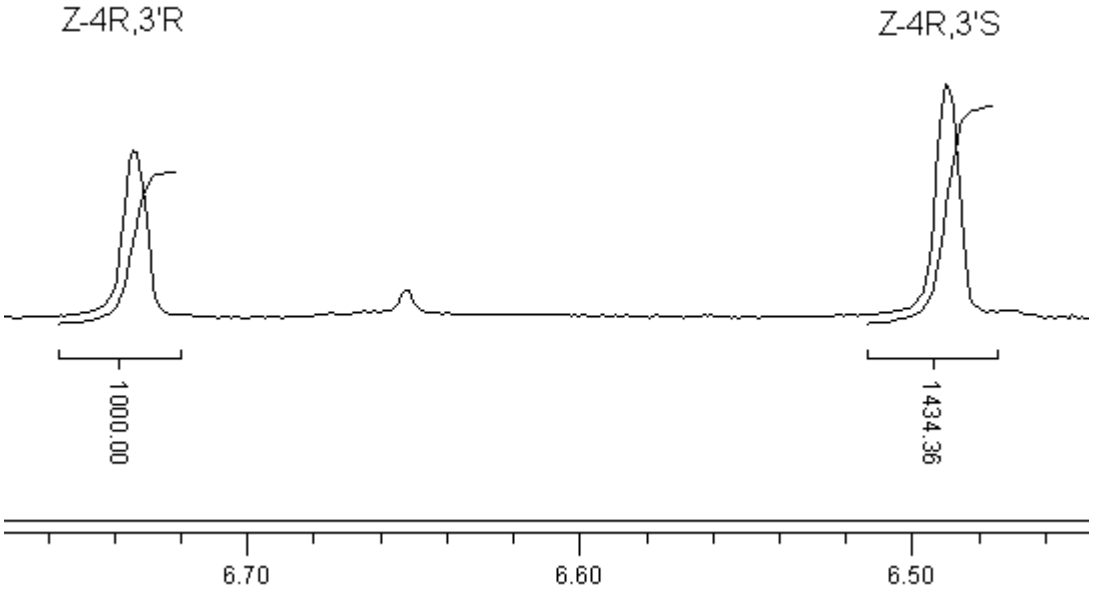

Figure 3.9.9. Trial 3, reaction of **1a** with PTAD (22.5 % conversion at -20°C in $CDCl_3$).

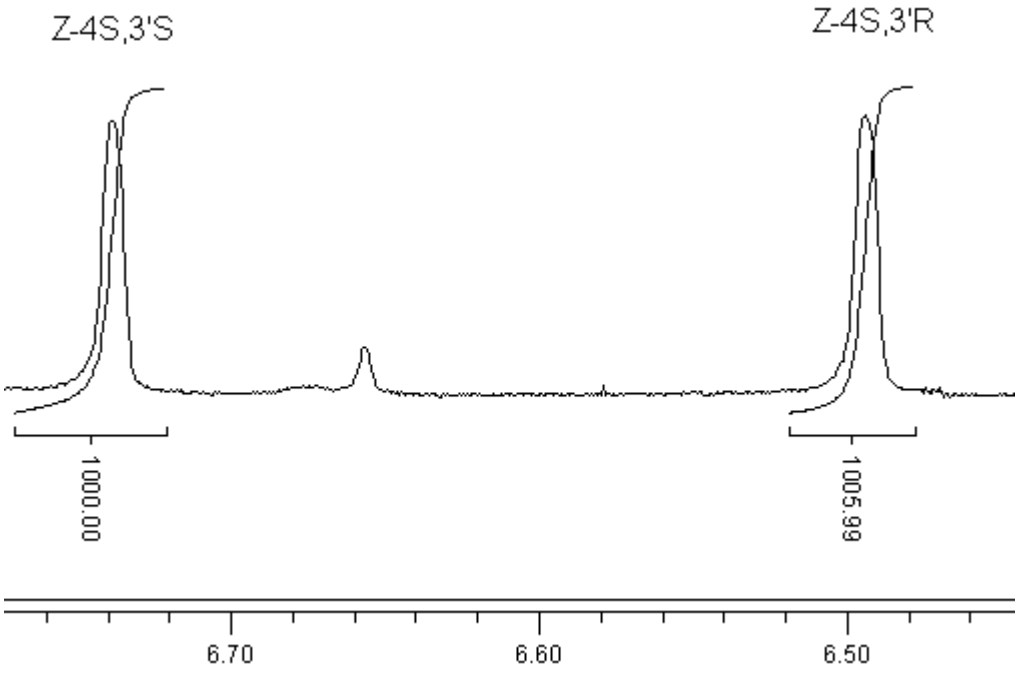

Figure 3.10.1. Trial 1, reaction of **1b** with PTAD (14.1% conversion at 24°C in $CDCl_3$).

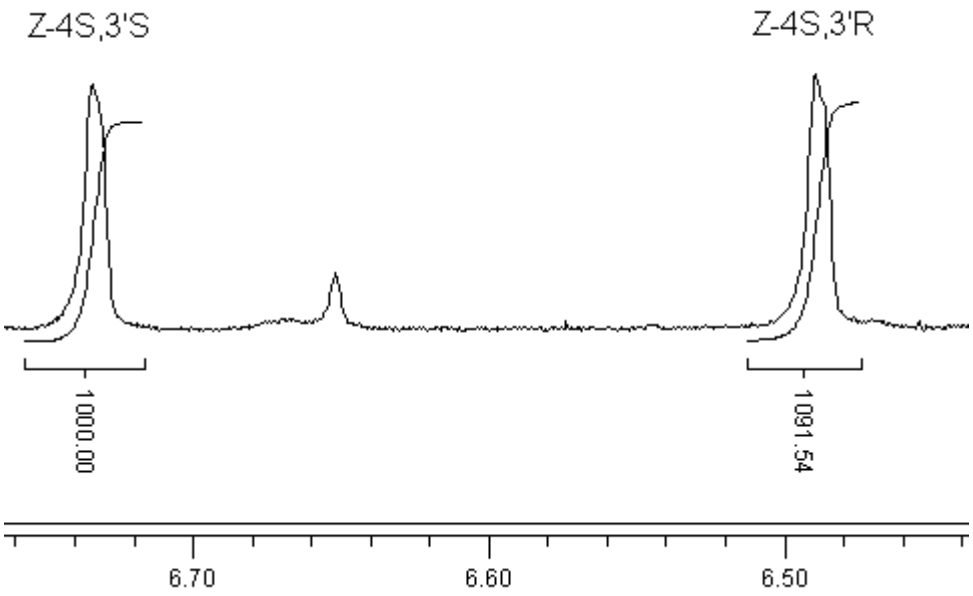

Figure 3.10.2. Trial 2, reaction of **1b** with PTAD (15.2% conversion at 24°C in $CDCl_3$).

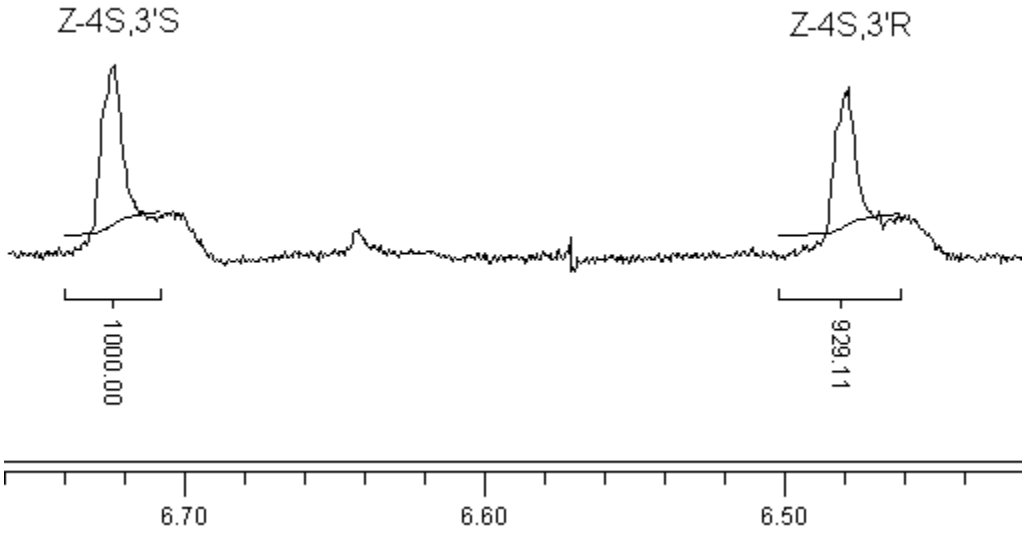

Figure 3.10.3. Trial 3, reaction of **1b** with PTAD (19.4% conversion at 24°C in $CDCl_3$).

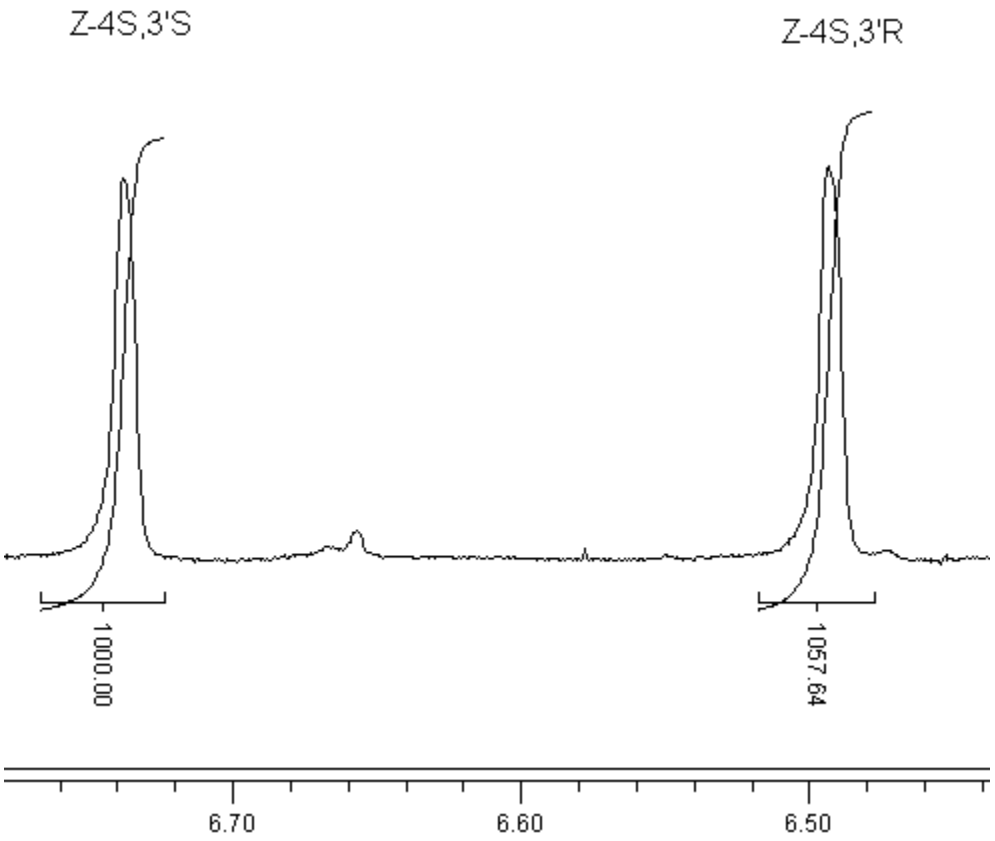

Figure 3.10.4. Trial 1, reaction of **1b** with PTAD (16.6% conversion at 7.0^{o}C in $CDCl_3$).

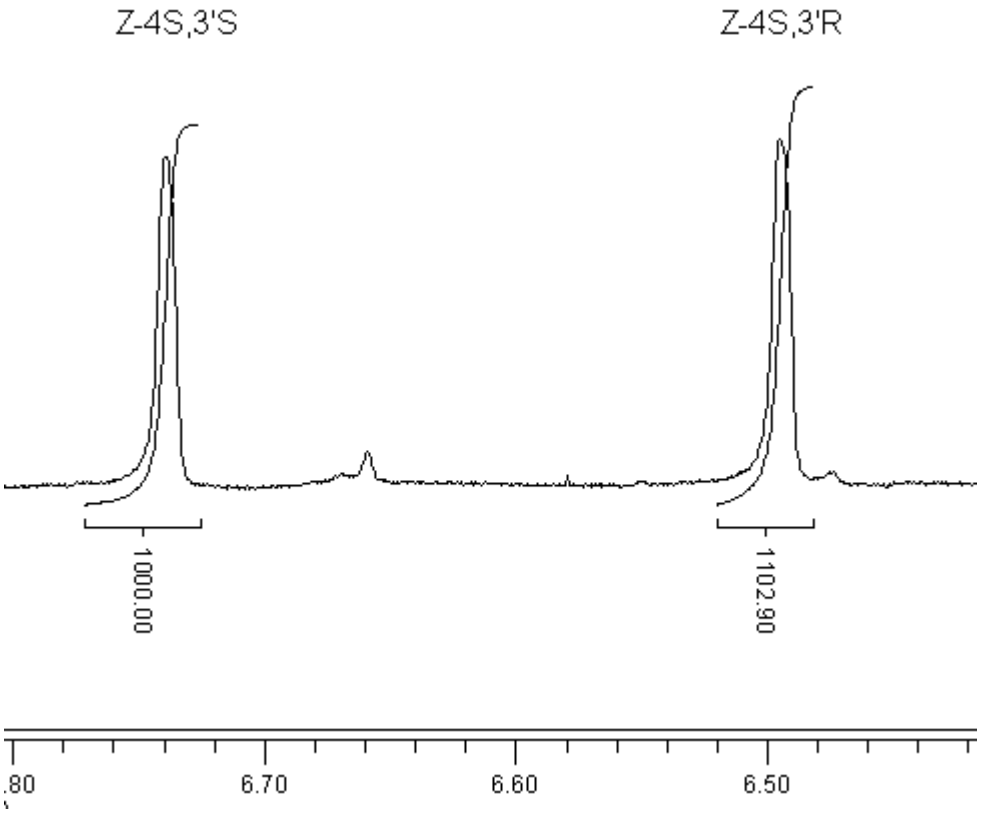

Figure 3.10.5. Trial 2, reaction of **1b** with PTAD (17.8% conversion at 7.0^{o}C in $CDCl_3$).

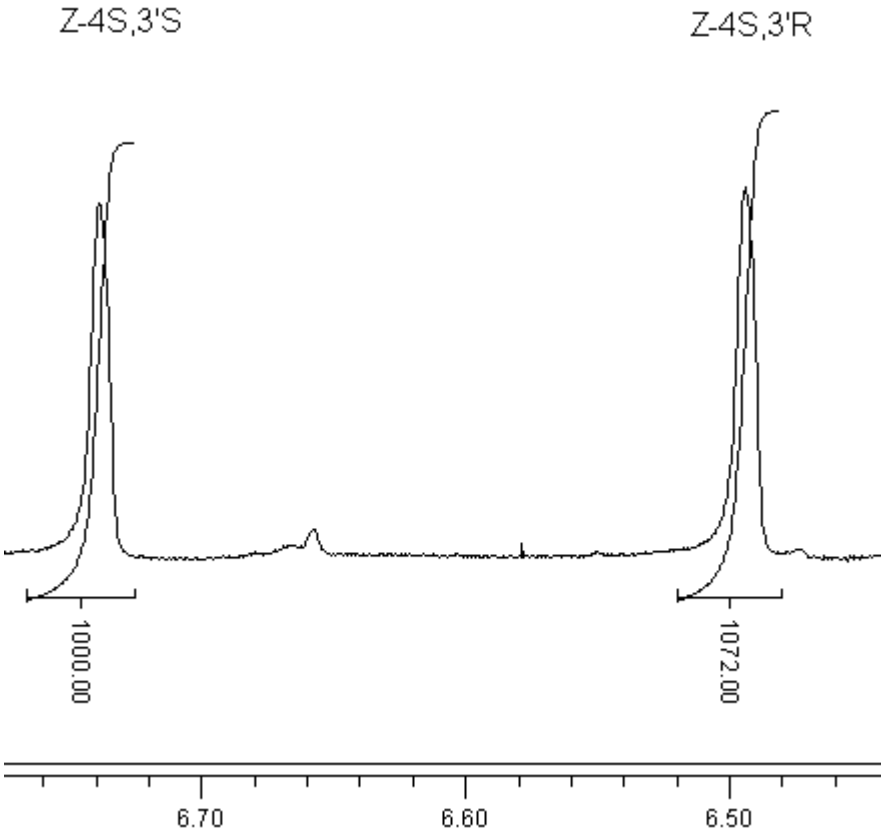

Figure 3.10.6. Trial 3, reaction of **1b** with PTAD (19.5% conversion at 7°C in $CDCl_3$).

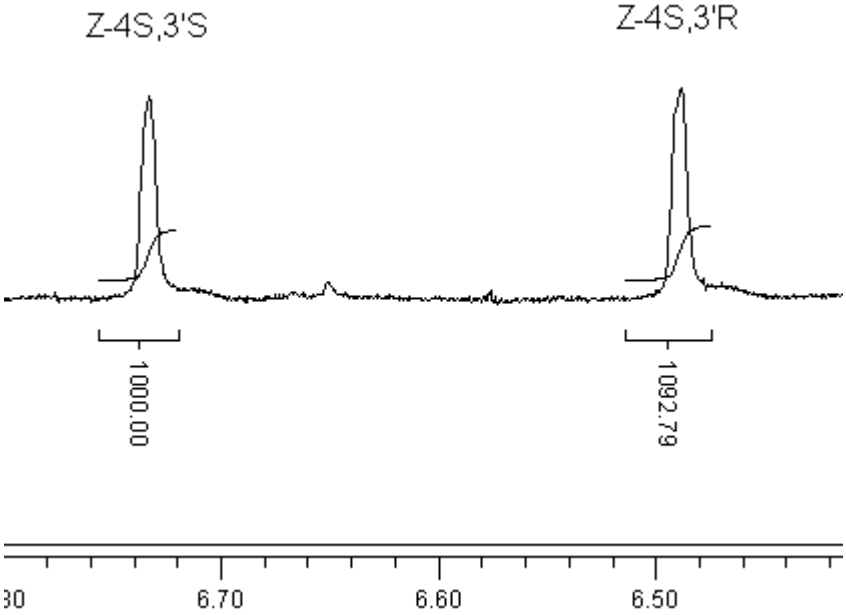

Figure 3.10.7. Trial 1, reaction of **1b** with PTAD (17.4% conversion at -20°C in $CDCl_3$).

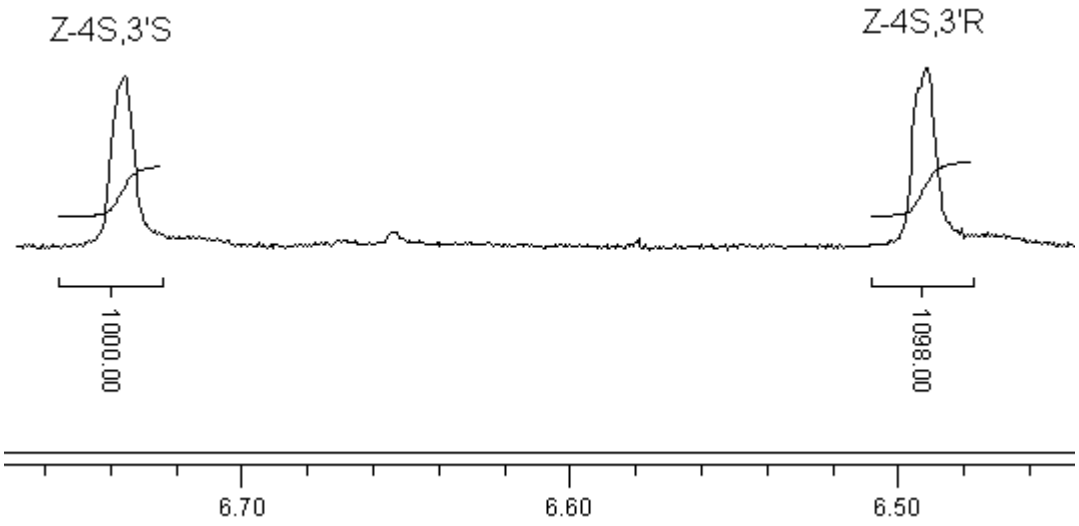

Figure 3.10.8. Trial 2, reaction of **1b** with PTAD (17.7% conversion at -20°C in $CDCl_3$).

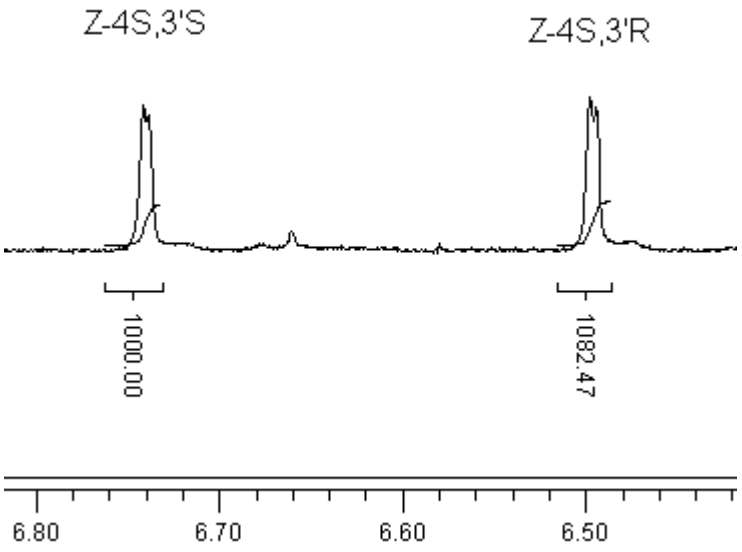

Figure 3.10.9. Trial 3, reaction of **1b** with PTAD (18.4% conversion at -20°C in $CDCl_3$).

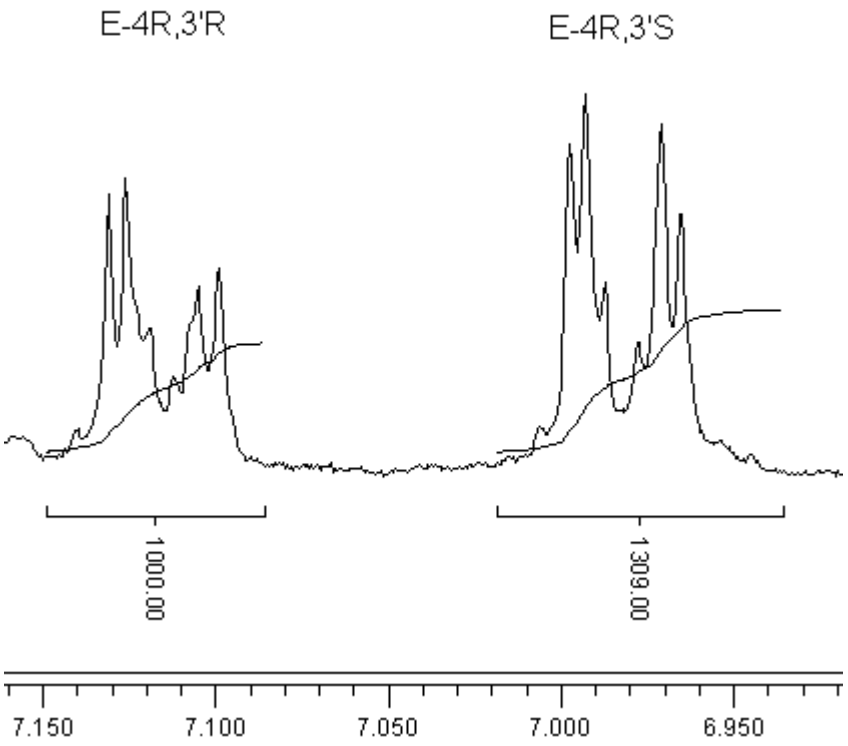

Figure 3.11.1. Trial 1, reacion of **1c** with PTAD (16.4% conversion at 24°C in $CDCl_3$).

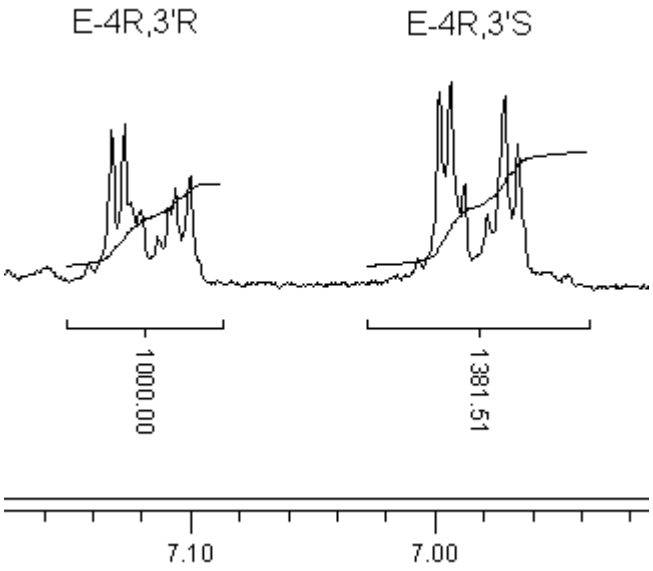

Figure 3.11.2. Trial 2, reacion of **1c** with PTAD (16.8% conversion at 24°C in $CDCl_3$).

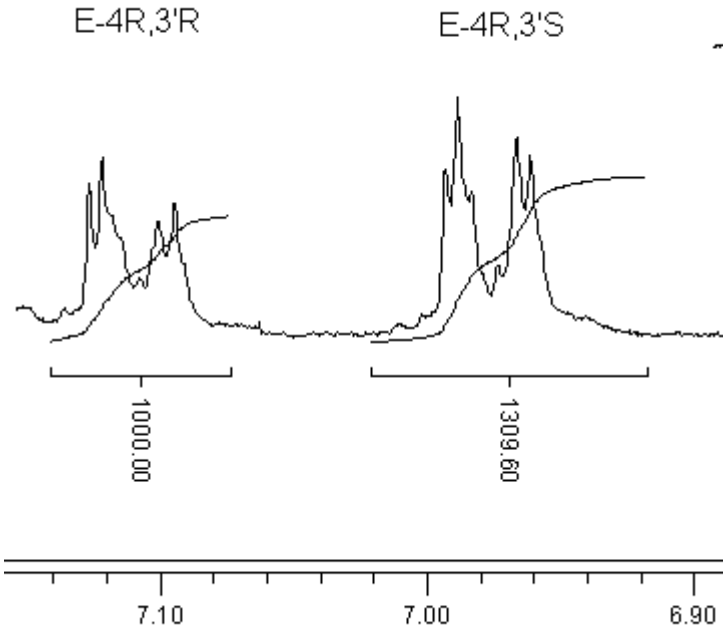

Figure 3.11.3. Trial 3, reaction of **1c** with PTAD (17.8% conversion at 24^{o}C in $CDCl_3$).

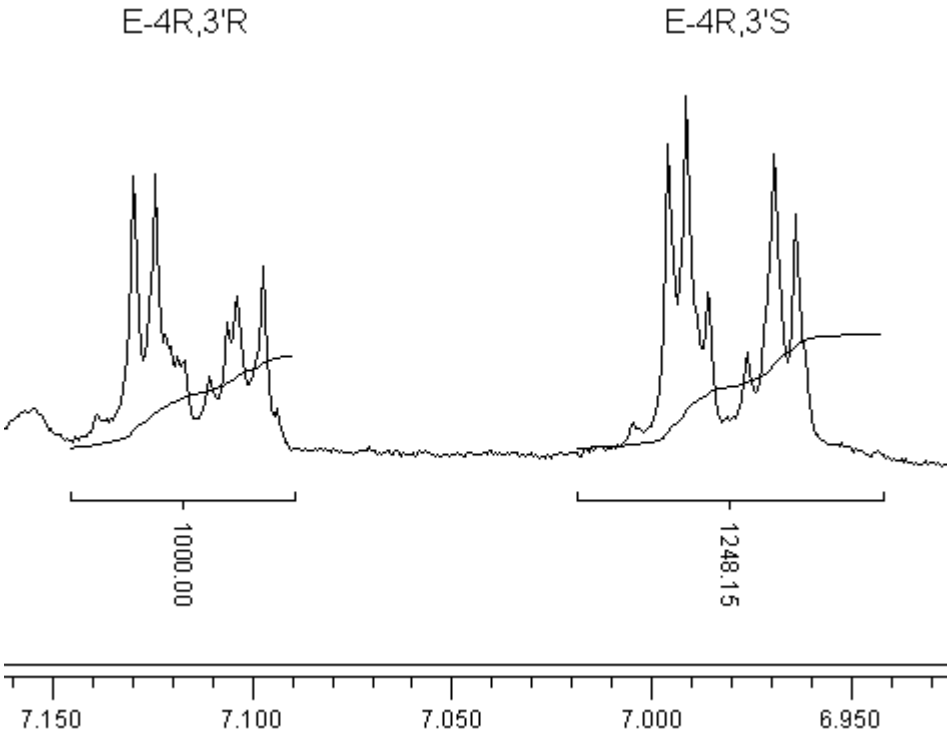

Figure 3.11.4. Trial 1, reaction of **1c** with PTAD (20.1% conversion at 7.0^{o}C in $CDCl_3$).

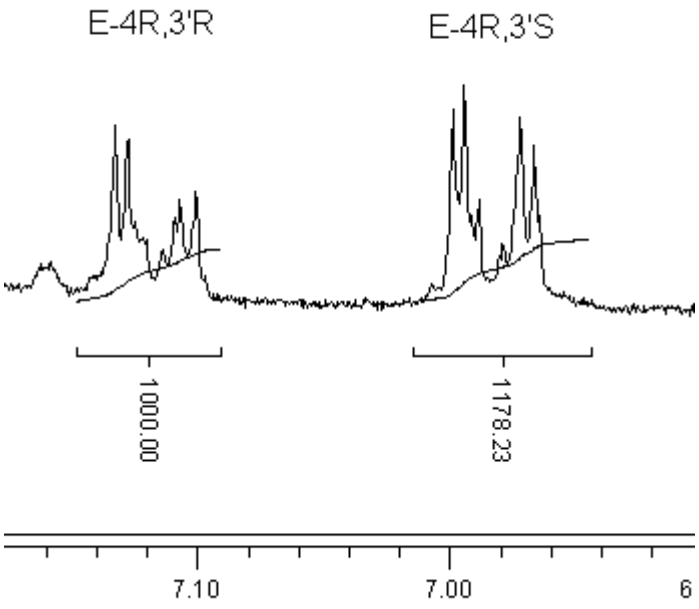

Figure 3.11.5. Trial 2, reaction of **1c** with PTAD (20.6% conversion at 7.0^{o}C in $CDCl_3$).

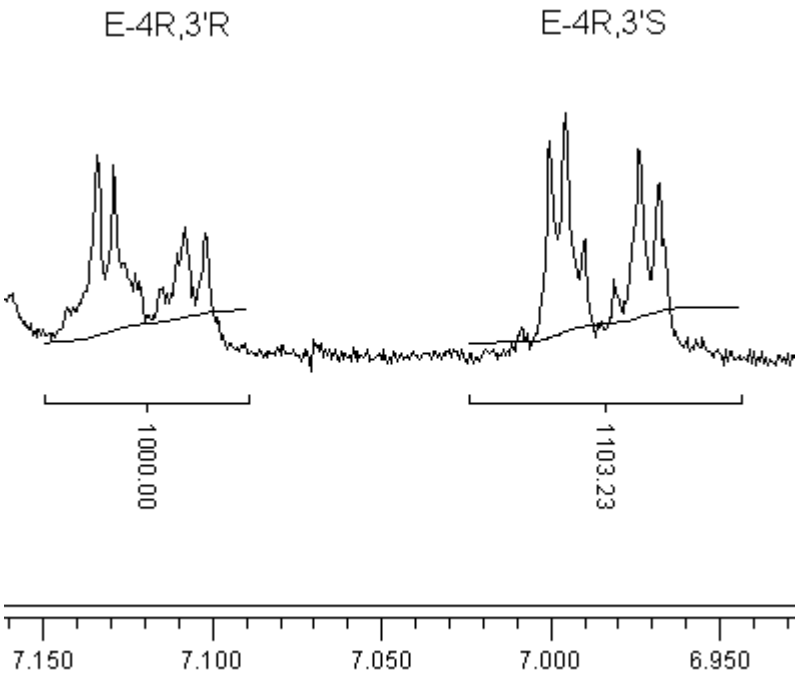

Figure 3.11.6. Trial 3, reaction of **1c** with PTAD (20.7% conversion at 7.0^{o}C in $CDCl_3$).

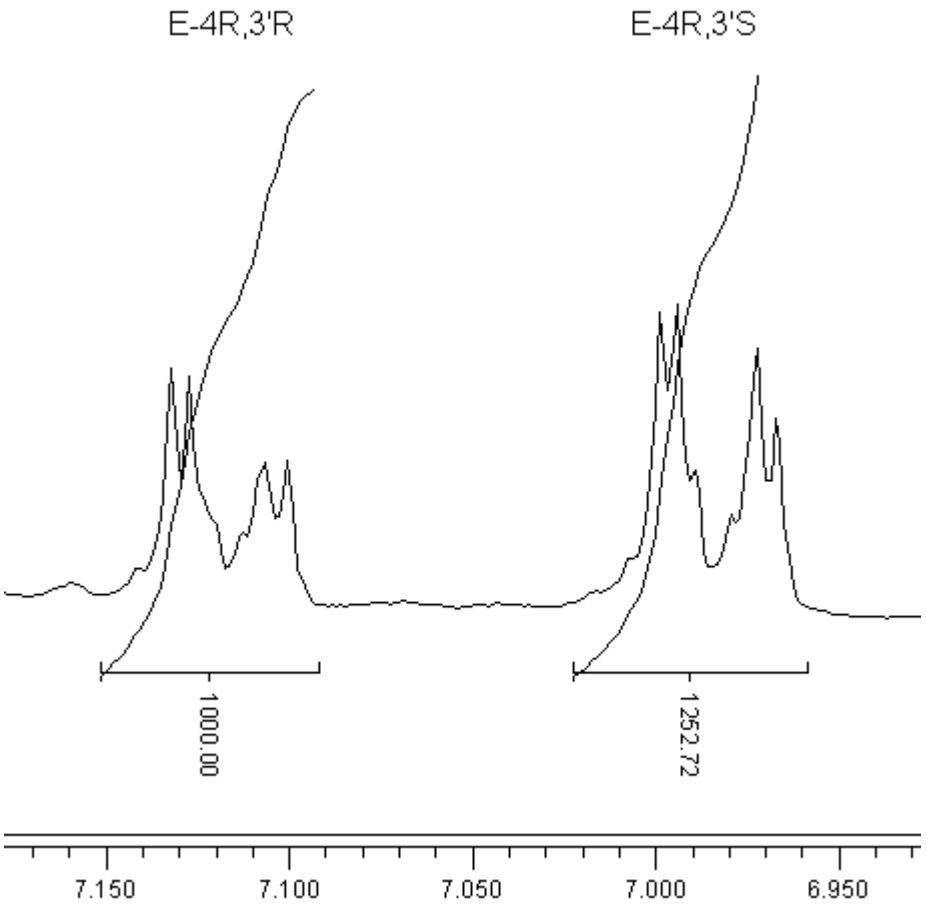

Figure 3.11.7. Trial 1, reaction of **1c** with PTAD (14.5% conversion at -20^{o}C in $CDCl_3$).

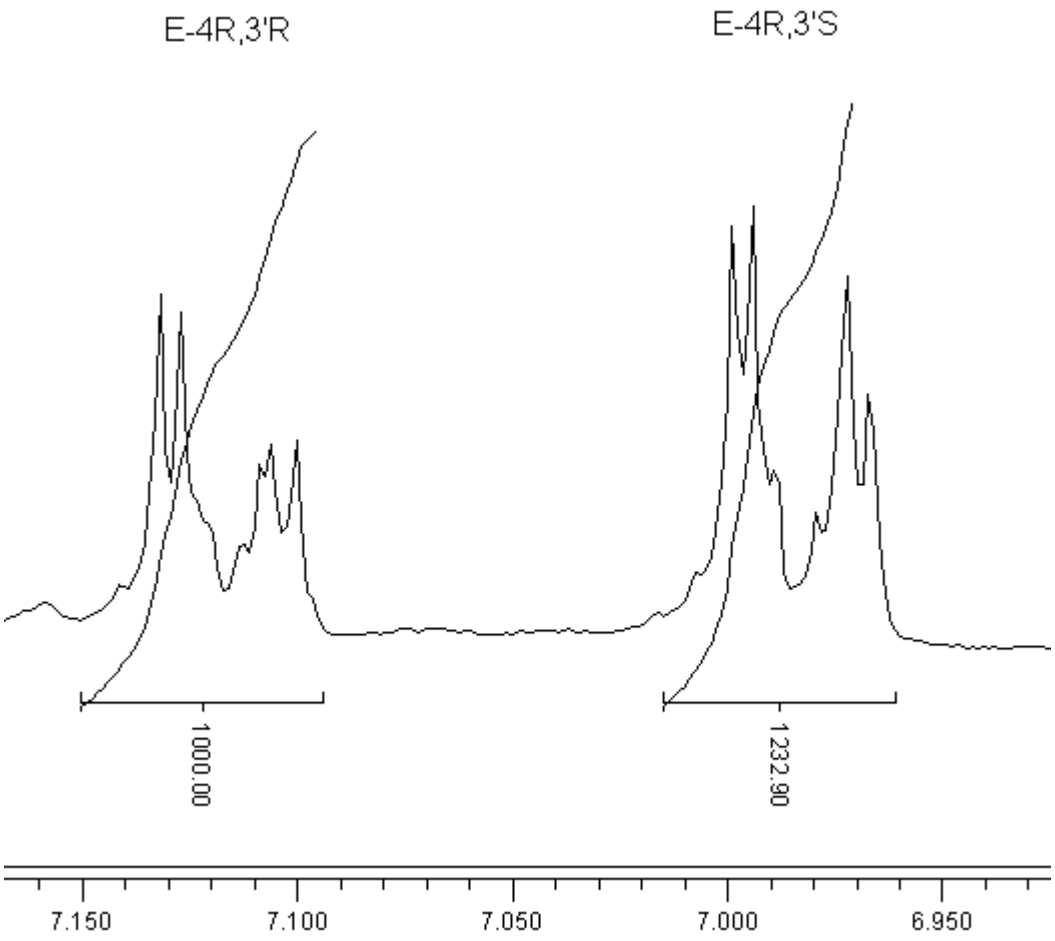

Figure 3.11.8. Trial 2, reaction of **1c** with PTAD (16.9% conversion at -20^{o}C in $CDCl_3$).

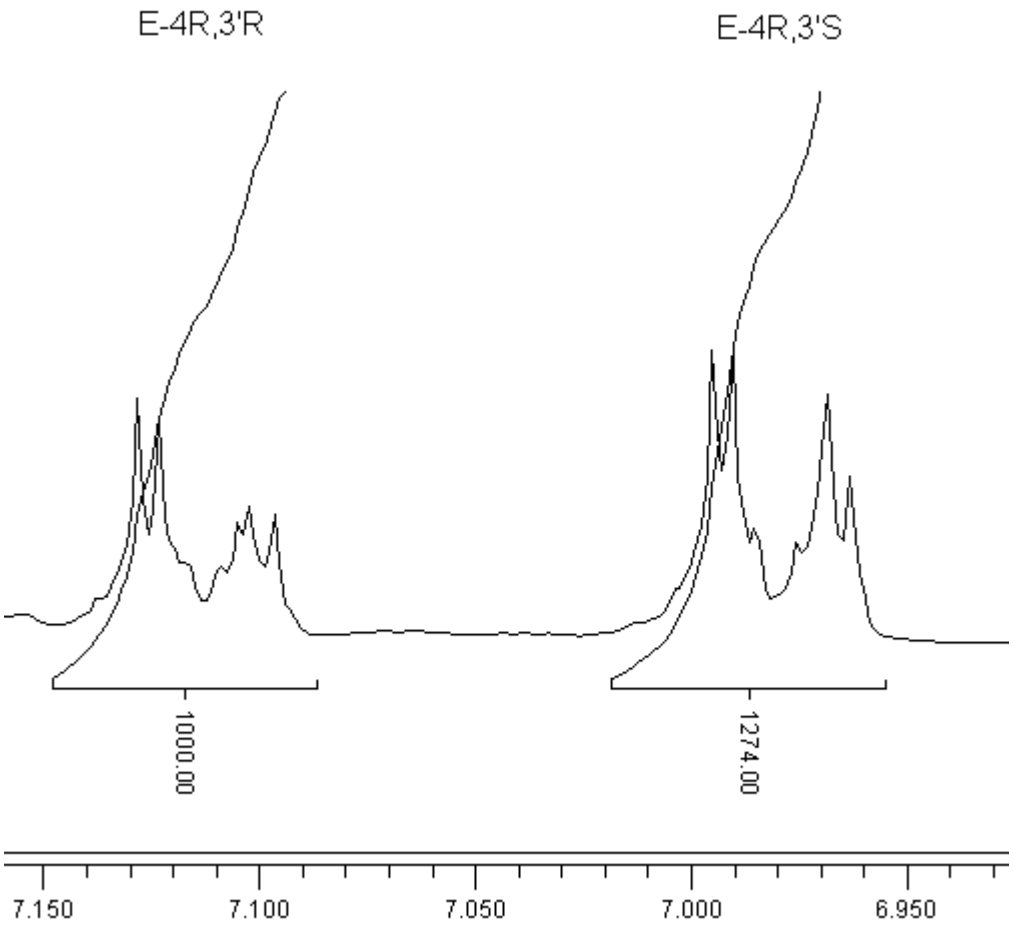

Figure 3.11.9. Trial 3, reaction of **1c** with PTAD (17.4% conversion at -20^{o}C in $CDCl_3$).

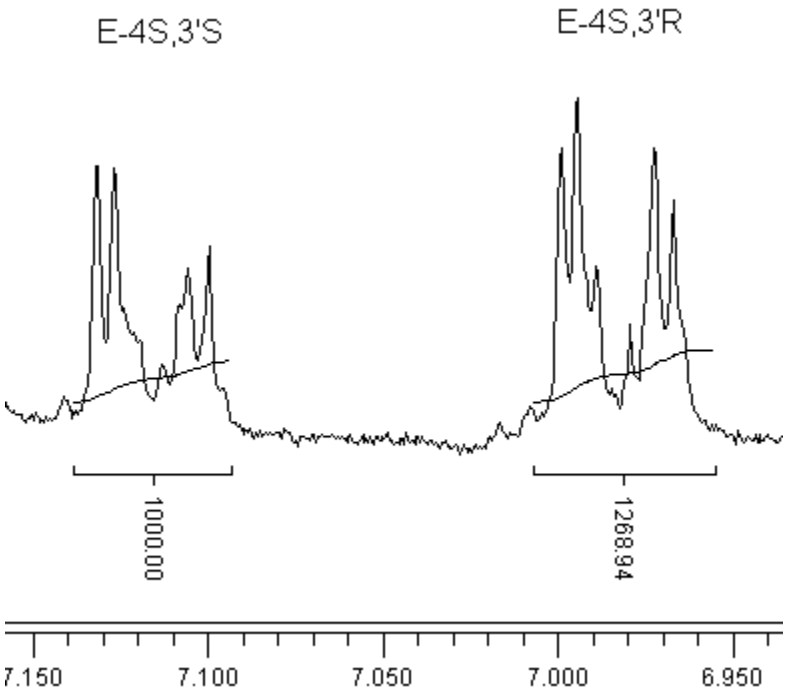

Figure 3.12.1. Trial 1, reaction of **1d** with PTAD (16.2% conversion at 24°C in $CDCl_3$).

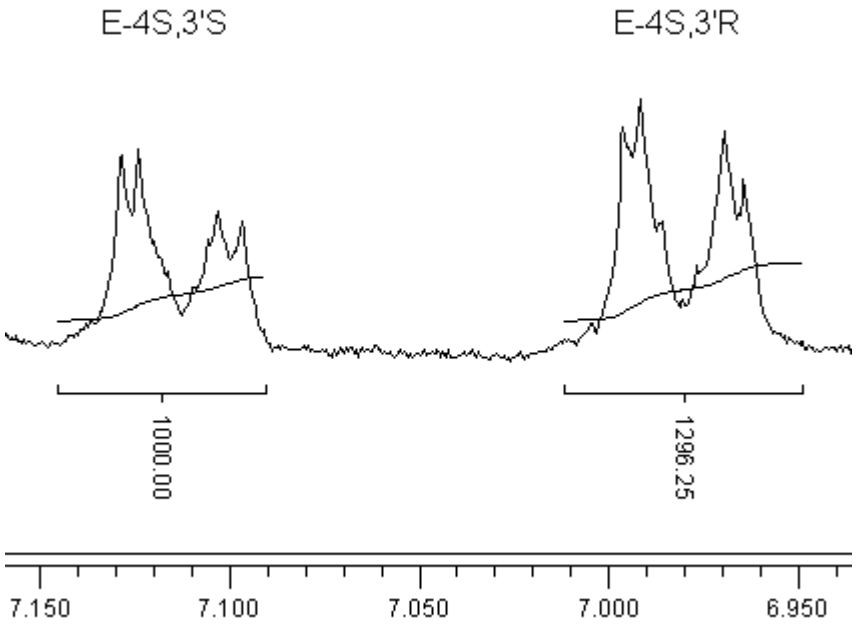

Figure 3.12.2. Trial 2, reaction of **1d** with PTAD (17.7% conversion at 24°C in $CDCl_3$).

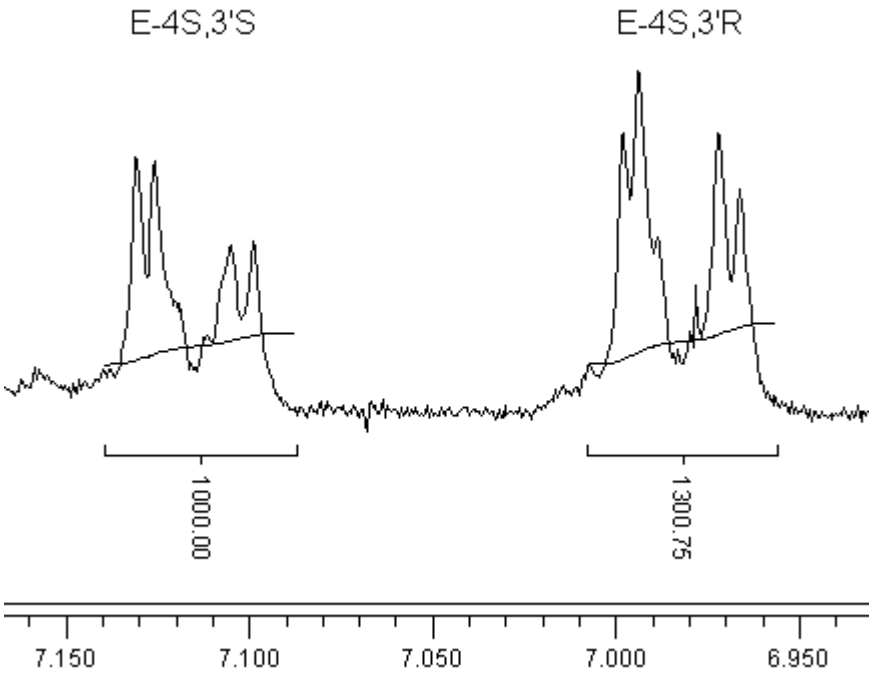

Figure 3.12.3. Trial 3, reaction of **1d** with PTAD (22.1% conversion at 24^{o}C in $CDCl_3$).

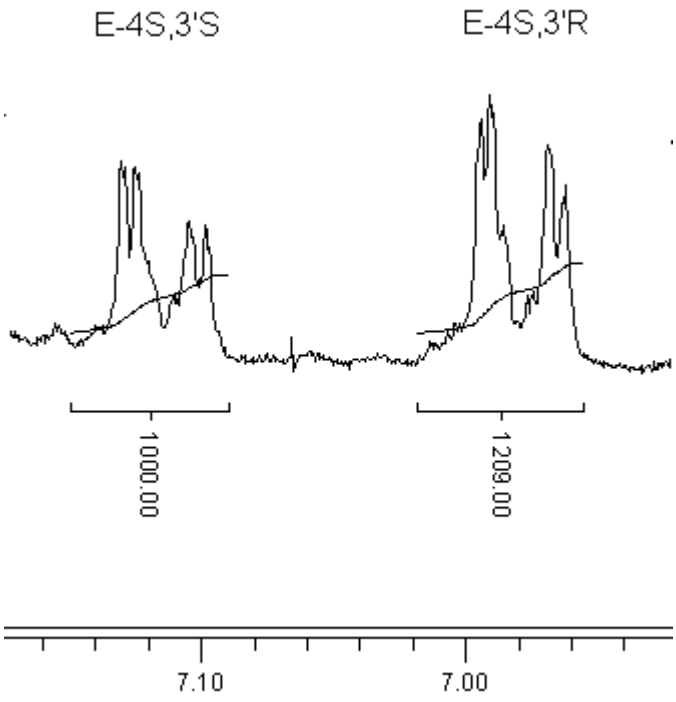

Figure 3.12.4. Trial 1, reaction of **1d** with PTAD (17.2% conversion at 7.0^{o}C in $CDCl_3$).

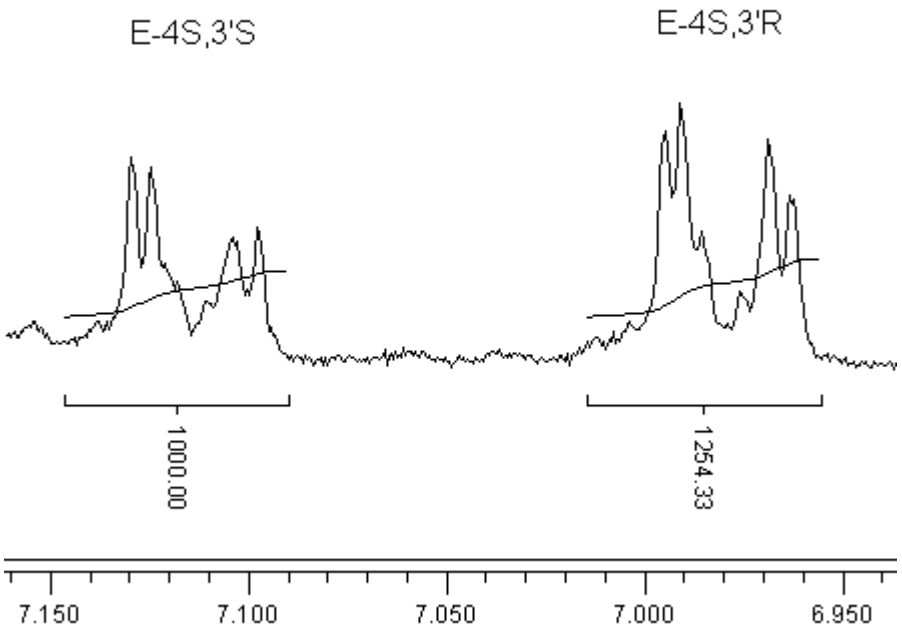

Figure 3.12.5. Trial 2, reaction of **1d** with PTAD (22.8% conversion at 7.0°C in $CDCl_3$).

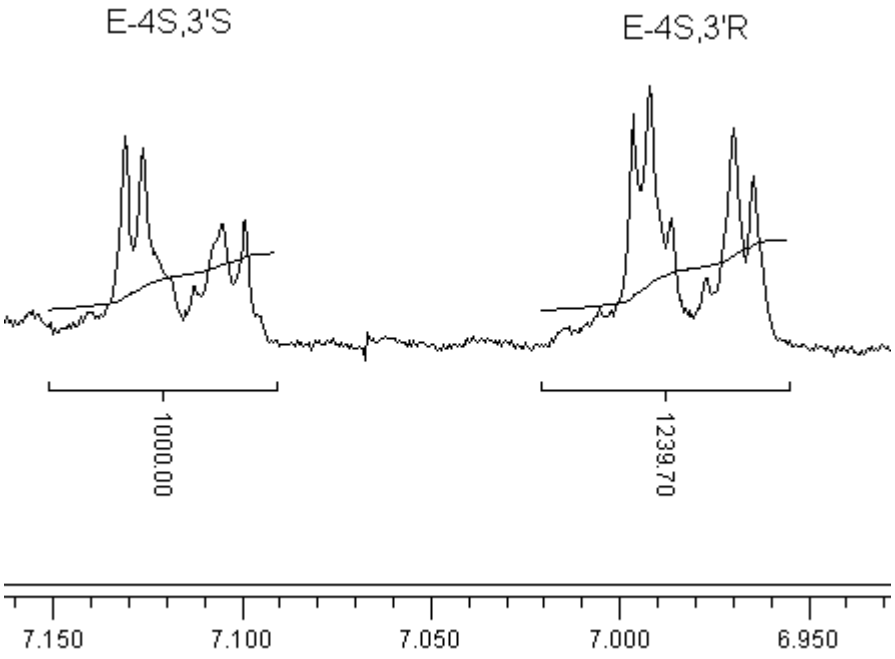

Figure 3.12.6. Trial 3, reaction of **1d** with PTAD (24.0% conversion at 7.0°C in $CDCl_3$).

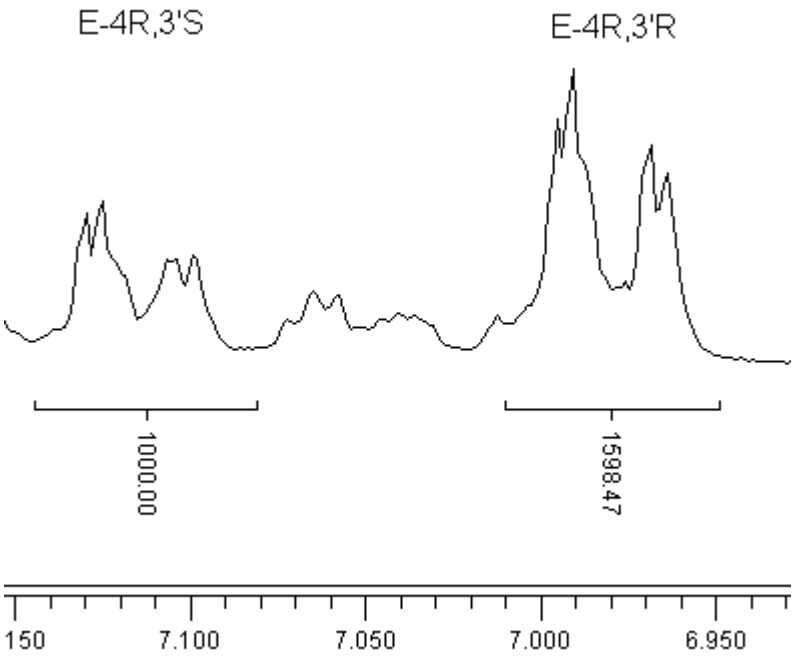

Figure 3.13.1. Reactions of **1c** with PTAD (10% conversion at 24^{o}C in $CDCl_3$).

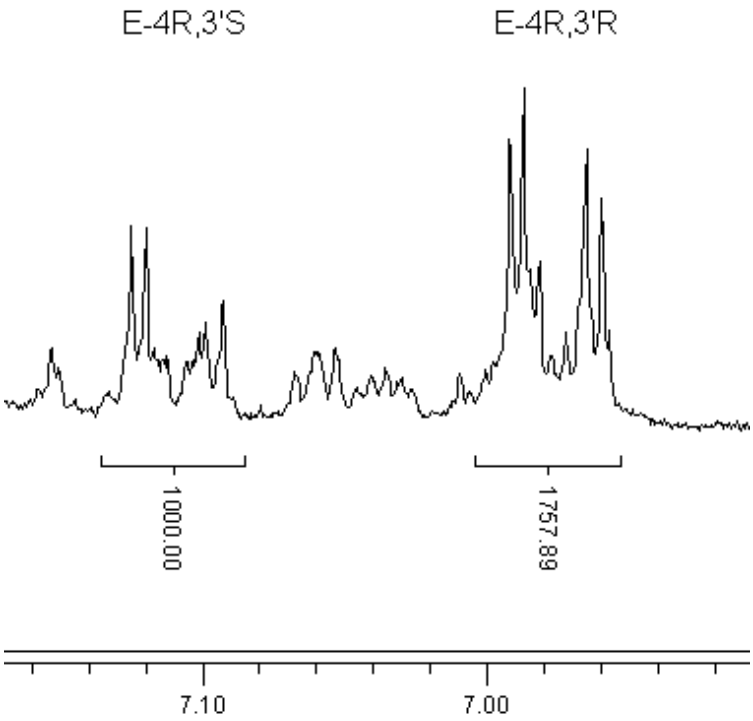

Figure 3.13.2. Reactions of **1c** with PTAD (20% conversion at 24°C in $CDCl_3$).

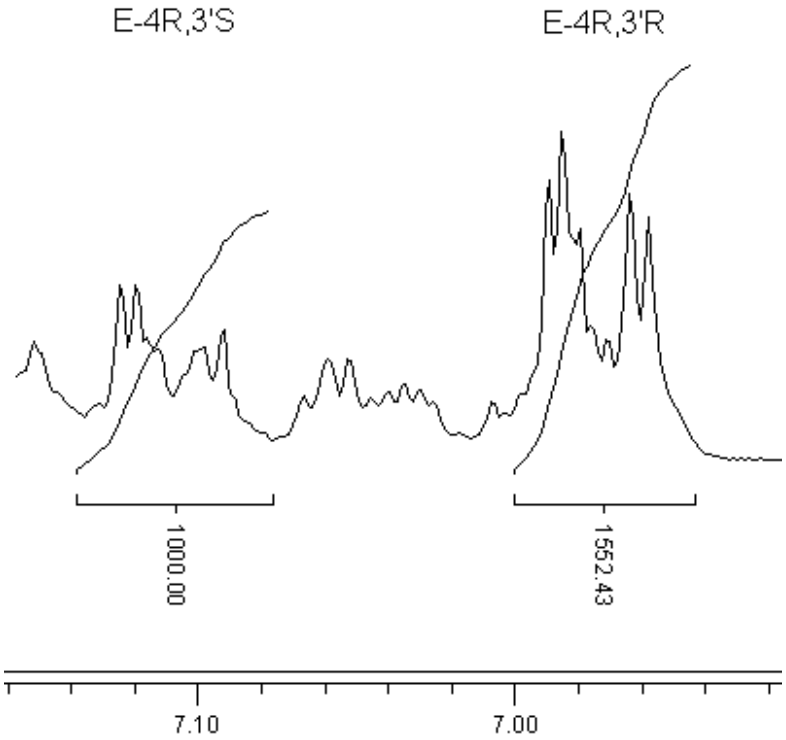

Figure 3.13.3. Reactions of **1c** with PTAD (40% conversion at 24°C in $CDCl_3$).

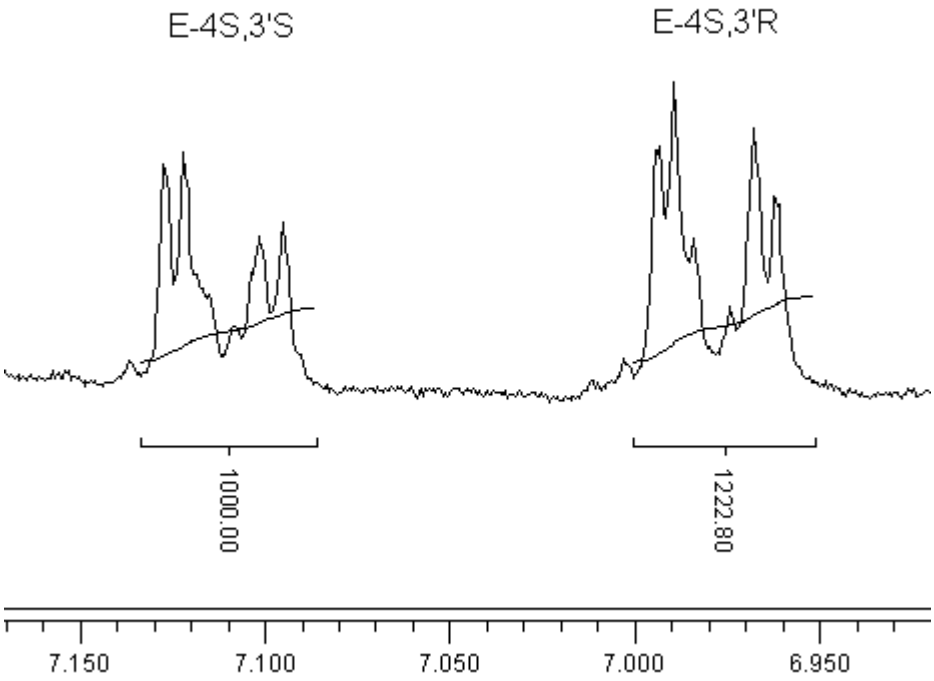

Figure 3.14.1. Reactions of **1d** with PTAD (10% conversion at 24°C in $CDCl_3$).

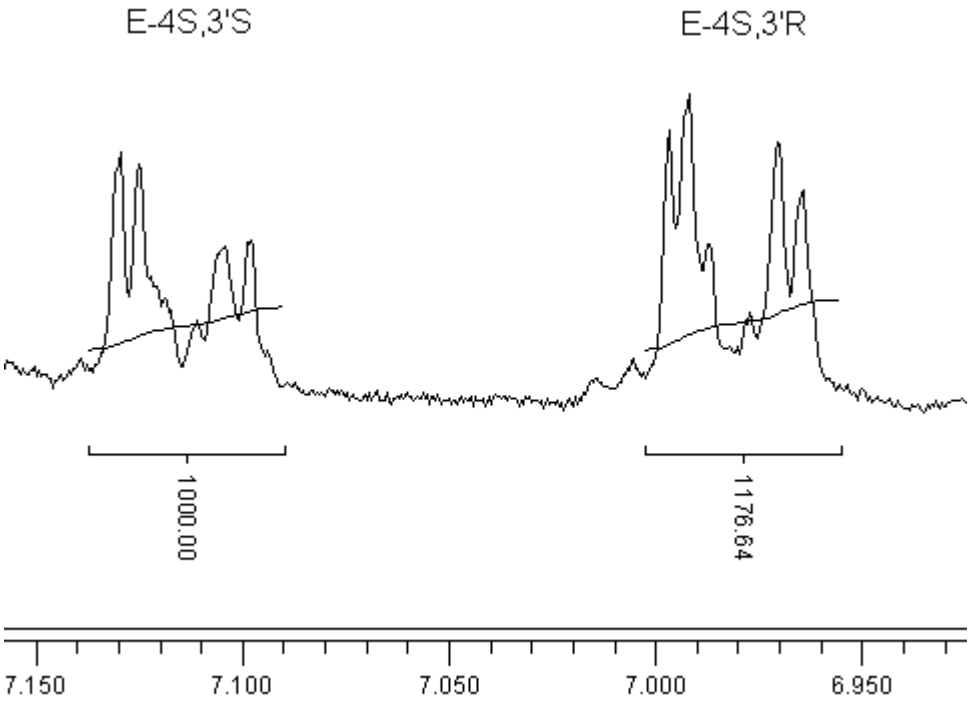

Figure 3.14.2. Reactions of **1d** with PTAD (20% conversion at 24°C in $CDCl_3$).

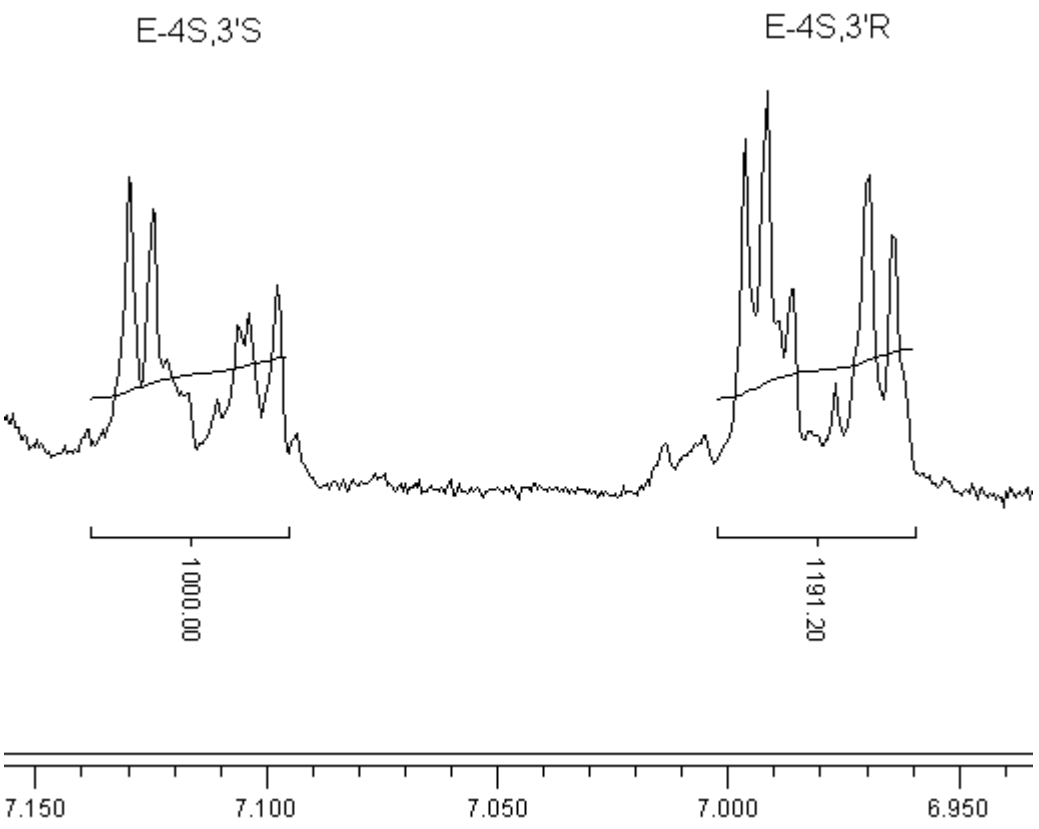

Figure 3.14.3. Reactions of **1d** with PTAD (40% conversion at 24°C in $CDCl_3$).

Chapter 4: Discussion

Diastereoselectivities of PTAD reactions with the enecarbamate are *much* lower than that seen with $^1O_2$ with no significant dependence on temperature. The species in diastereotropic excess (%d.e.) is the species with the less favorable C-3' conformation causing it to react slower with PTAD. Low d.e. values indicate that neither diastereomer is significantly more reactive with the PTAD molecule. Due to the bulkiness of the molecule and the fact it exists in a ground state, any selectivity found in the PTAD reactions can be attributed to differing degrees of steric interference at chiral centers. The fact that there is a much higher selectivity with the $^1O_2$ than with the PTAD reactions suggests that there are other contributing factors beyond sterics that drive the selectivity of the singlet oxygen reactions.

Singlet oxygen shows highest selectivity when reacting at low temperatures in CD_3OD.[13] Given the nature of PTAD and the high reactivity of its reaction intermediates with alcohols, CD_3OD could not be used as a solvent.[16] Reactions of singlet oxygen with **1c** or **1d** in CD_2Cl_2, $CDCl_3$ or CD_3CN show moderate to hight selectivity along with a strong dependence on solvent and temperature (Table 1.2). As previously indicated, limited amounts of starting materials precluded our ability to explore these solvent effects.

The data in Table 3.1 suggests that higher diastereoselectivity will not be achieved when decreasing the temperature (even to those degrees explored in the singlet oxygen reactions). Selectivity of **1a** reacting with singlet oxygen in $CDCl_3$ when the reactions are allowed to go to 50% conversion is only around 30% at 24^{o}C (Table 1.1),

however, this is far more selective than what was found in the PTAD reactions (averaging under 14% at –20°C and only about 18% conversion average, Table 3.1). As is shown in Tables 3.6 and 3.7, reaction selectivity decreases with increased reaction conversion. This is logical: if a reaction goes to 100% conversion, there would be no selectivity because by the time a reaction reaches completion, both species of the epimeric mixture will be converted to their respective products. Consequently, the closer a reaction gets to reaching 100% completion, the less likely it is the data will show a reaction preference of one diastereomer over the other.

The fact singlet oxygen is exhibiting a significantly higher selectivity than PATD indicates that there are different modes of reactivity in operation between these two enophiles. The PTAD reaction with **1a** did show slight temperature dependence in that when the temperature decreased, the selectivity increased. This increase however, was so small that the standard deviations among the trials taken could account for the spread of data. In the end it must be concluded that the temperature did not help increase selectivity of **1a** with PTAD.

The same analysis holds for singlet oxygen and PTAD reactions with **1b**. When reacting with **1b** and **1d**, singlet oxygen still observed higher selectivity than that found in the PTAD reactions (Table 1.1). Although singlet oxygen shows only slight selectivity when reacting with **1b** (11%e.e. at 47% conversion in $CDCl_3$ at 24°C, Table 1.1), this is still more than what is found in the PTAD reactions at lower temperatures in the same solvents (averaging under 8% d.e. at its most selective point at 7°C at about 18% conversion average, Table 3.2). The argument that steric effects do not play a large role in stereodifferentiation in the $^1O_2$ reactions is supported by these results.

Reactions with $^1O_2$ and **1c** showed highest diastereoselectivity in CD_3OD at temperature of –40°C (94%e.e.).[13] Comparative selectivity between singlet oxygen and PTAD is easily determined by looking at the reactions carried out in $CDCl_3$. The lower selectivity exhibited by PTAD compared to $^1O_2$ also suggests that when reacting with **1c,** $^1O_2$ selectivity is not due to steric interferences. As with the Z-enecarbamates (**1a** and **b**),varying the temperature does not a role in the reaction selectivity (Table 3.3).

Comparing Table 1.2 to 3.4 shows the degree to which singlet oxygen is better able to stereodifferentiate when reacting with **1d**. Even though it is in CD_2Cl_2 rather than $CDCl_3$, $^1O_2$ never observes e.e. values under 28% at its warmest temperature (18°C at almost 30% conversion), and observes 88% e.e. at its lower temperatures (-60°C at 56% conversion). PTAD d.e. values for the **1d** reactions never reached above 13.1% at conversions as low as 22.1%. This again supports to **1b,** just as seen in **1a-c,** that selectivity observed by $^1O_2$ is not driven by sterics.

Even though $^1O_2$ shows much higher selectivity than PTAD, both singlet oxygen and PTAD are selecting for the same diastereomers (as did O_3).[13] This permits an argument for the connection between physical and chemical quenching. It is the dramatic difference in selectivity of PTAD and $^1O_2$ when reacting with **1a-d** that strongly supports the hypothesis that selectivity of $^1O_2$ is due to vibrational deactivation rather than sterics. Because PTAD is a much larger enophile than $^1O_2$, its low selectivity with enecarbamates **1a-d** suggests that sterics do not contribute significantly to the differentiation seen in these types of reactions. Physical quenching cannot drive selectivity with PTAD reactions because, unlike $^1O_2$, PTAD is a ground state molecule. "This proves that the high stereoselectivity observed for $^1O_2$ (~97% ee at –70°C; CD_3OD; Table 1.2) relates

presumably to its electronically excited nature, since it may be vibrationally deactivated on encountering C-H bonds.[11, 12] Figure 4.1 below demonstrates these interactions with respect to **1a**.

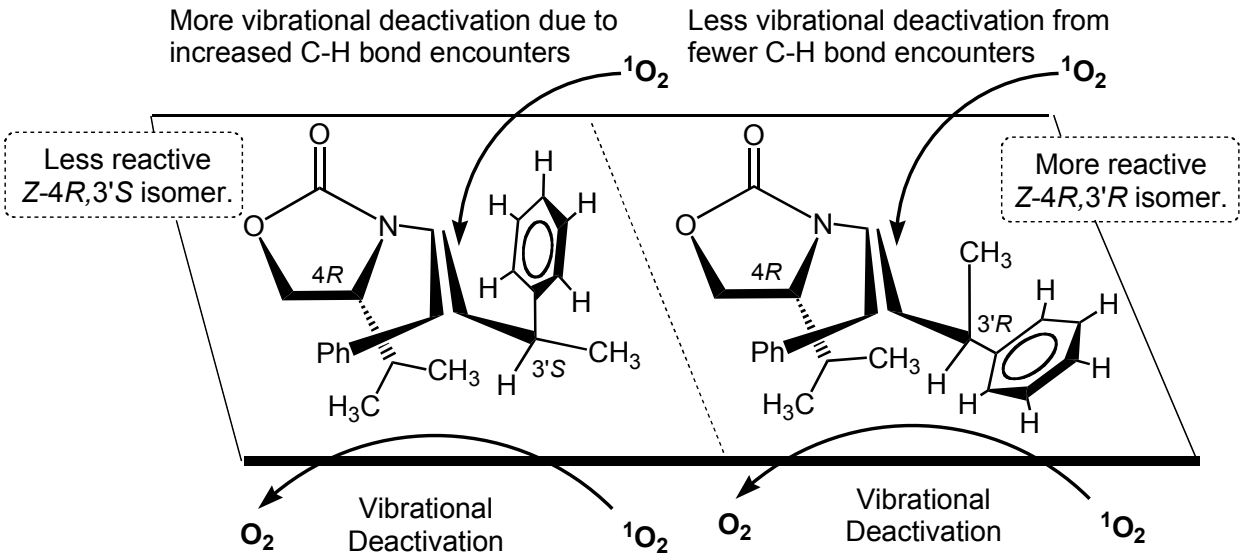

Figure 4.1. Vibational deactivation between $^1O_2$ and **1a** driven by C-H bonds at C-4 and C-3'.

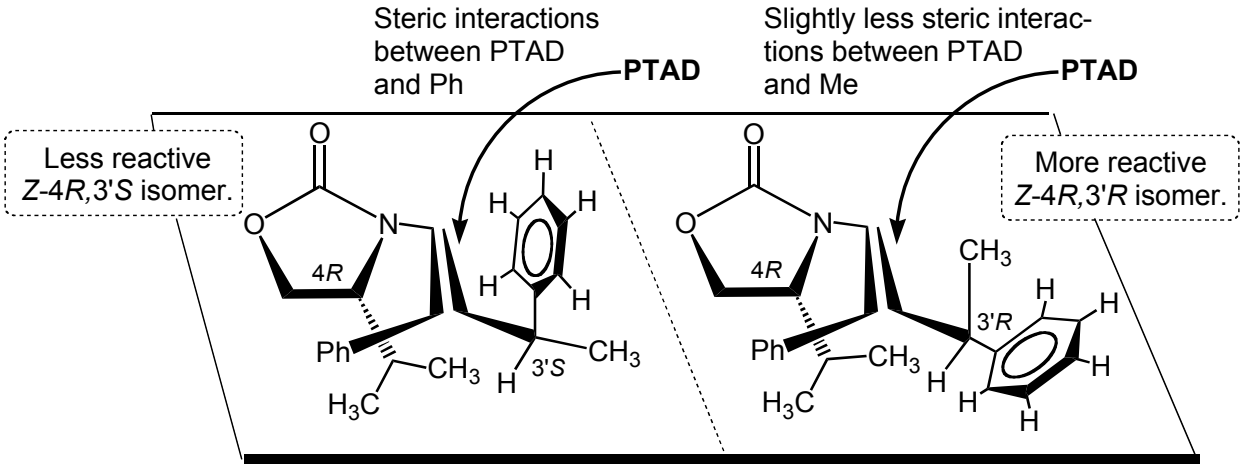

Figure 4.2. Steric hindrance due to C-4 and C-3' drives *slight* selectivity found in the PTAD and **1a** reactions.

As Figure 4.1 shows, and as was determined earlier though the work with ozone (see appendix), the isopropyl group and its orientation at C-4 is responsible for blocking

the attack of $^1O_2$ from what is displayed as the bottom side of the molecule. The two methyl groups of this chiral auxiliary provides an abundantly furnished "shield" of C-H bonds that deactivate the $^1O_2$ with their vibrational energies.

The C-3' position of the oxazolidinone chiral auxiliary is now better understood through the results presented in the PTAD reactions. The phenyl group at the chiral center of interest did not direct enough selectivity when reacting with the bulky PTAD to support an argument of steric hindrance in the $^1O_2$ reactions. As Figure 4.2 above depicts for PTAD, sterics is only a small contributing factor to the low selectivity found in these reactions. It now appears that a physical quenching from the vibrational energy of the C-H bonds plays a more important role in the stereoselectivity of the $^1O_2$ reactions. Pertaining to Figure 4.1 above, it is obvious that there is a greater abundance of C-H bonds when the C-3' has the S configuration. Data shows that it is also this isomer that $^1O_2$ is less reactive with, oxidizing the 3'R isomer more readily given the decrease in the number of vibrationally deactivating C-H bonds existing with the methyl group in place of the 3'S phenyl group. Experiments at Columbia are underway to further support this hypothesis. If those C-H bonds are replaced with C-D bonds, the reduction in vibrational frequencies should directly affect the selectivity of **1a, b, c,** and **d** with $^1O_2$. One should expect that lowering the vibrational energies of those bonds at the chiral point of interest (C-4 and C-3') will decrease selectivity. Since a deuterium atom is heavier than a hydrogen atom, the vibrational energy between a C-D bond will be less than that of the C-H bond, supplying a smaller, less favorable, energy scale for the excited oxygen to transfer its energy to upon deactivation.

Chapter 5: Conclusion

Original understanding of steric driven stereodifferentiation of $^1O_2$ has been challenged through the study of PTAD and its selectivity on oxazolidinone substituted enecarbamates. Extensive studies have been done to this point with these chiral auxiliaries and $^1O_2$, finding that selectivity of the photooxidation reaction can reach %e.e. values of 94%. While singlet oxygen is known to be one of the smallest more reactive enophiles, PTAD, which reacts via the same mechanism is bulky and would exhibit enormous selectivity if sterics was the driving factor solely based on the large size of the bulky molecule. This however was not the case. Little to no selectivity was seen in the PTAD reactions with **1a-d** at varying temperatures in $CDCl_3$. This was displayed through the low d.e. values of all the PTAD reactions carried out. At this point, steric quenching no longer fully accounts for the unique selectivity of singlet oxygen. Rather, it is most likely physical quenching caused by the C-H bonds at the C-3' chiral position of **1a-d** that is preventing $^1O_2$ from reacting with the double bond.

References

([1]) Nelson, David L.; Cox, M. M.; Lehninger. "Principles of Biochemistry," 4th edition, W. H. Freeman and company, New York, NY. **2005**

(2) "PDT Cancer Treatment Program." Oregon Medical Laser Center ON PDT Cancer Treatment Program. **1 Jan.1999**. Organ Medical Laser Center. 5 Dec. 2004 <http://omlc.ogi.edu/pdt/index.html >.

(3) Zhao, Lingijie. "Singlet Oxygen: Free Radical and Radiation Biology Graduate Program Department of Radiology." Ph.D. Dissertation. Unpublished. **2001**

(4) Fouad, Tamer. "Free Radicals, Types, Sources and Damaging Reactions." www.thedoctorslounge.net/medloung/articles/, Singlet Oxygen. **2004**

(5) Adam, W.; Mielke K.; Saha-Möller, C.; Möller, M., Stopper, H.; Hutterer, H., Scheinder, F.; Ballmaier, D.; Epe, B.; Gasparro, F.; Chen, X.; Kagan, J. "Photochemical and photobiological studies of Furonaphthopyranone as a Benzo-spaced Psoralen Snalog in Cell-free and Cellular DNA." *Photochemistry and Photobiology* **1997**, 66/1

(6) Grossweiner, Leonardo I.. "Singlet Oxygen: Generation and Properties." Wenske laser center, advocate/ Ravenswood hospital medical center. 5 Nov. 2004. http://www.photobiology.com/educational/len2/singox.html.

(7) Wolfgang, Johann. "Photophysics and Photochemistry of Singlet Oxygen – a Very Special Area." Institut für Physikalische und Theoretische Chemie. 18 Apr.2005. http://user.uni-frankfurt.de/~rsch/1O2-english.html.

(8) Adam, Waldemar; Guthlein, Markus; Peters, E.-M.; Peters, Karl; Wirth, Thomas. "Chiral-Auwiliary-Induced Diastereoselctivity in the [4 + 2] cycloaddition of optically active 2,2-Dimethyloxaolidine Derivatives of Sorbic Acid; A Model Study with Singlet Oxygen as the Smalles Dienophile." *J. Am. Chem. Soc.* **1998**, 120.

(9) Schulte-Elte, K H.; Muller, B. L.; Rautenstrauch, B. 264. Preference of Syn Ene Addition of $^1O_2$ to Trisubstituted Acyclic Olifins *Helv. Chim. Acta* **1978**, 61, 2777.

(10) Adam, Waldemar; Chantu R. Saha-Moller; Simon B. Schambony. "A Highly DIastereoselective Dioxetane Formation by the Hydroxy-Directed [2 + 2]

Cycloaddition of Singlet Oxygen to a Chiral Allylic Alcohol." *J. Am. Chem. Soc.* **1999,** 121

(11) Vassilikogiannakis, Gorgios, Manolis Stratakis, Micheal Orfanopoulos Christopher S. Foote. "Steroschemistry in the ene reactions of singlet oxygen and triazoliediones with allylic alcholoes." A mechanistic comparison *J. Org. Chem.* **1999,** 64.

(12) Adam, Waldemar; Peters Karl; Peters, Eva-Maria; Schambony, Simon B. "Diastereoselective and Regioselective Singlet-Oxygen Ene Reactions of Oxazolidine-Substitued Alkenes: Control through Hydrogen Bonding Mediated by the Urea Functionality of Chiral Auxilaries." *J. Am. Chem. Soc,* **2000,** 122.

(13) Poon, Thomas, J. Sivaguru, R. Franz, S. Jockusch, C. Martinez, I. Washington, W. Adam, Y. Inoue, Turro, N. J. "Multidimensional Control of Stereoselectivity in the Reactions of Singlet Oxygen with Oxazolidinone-substituted Enecarbamates." *J. Am. Chem. Soc.* **2004**126: 10498-10499.

(14) Poon, Thomas; Turro, Nicholas J.; Chapman, Jessica; Lakshminarasimhan, P.; Lei, Xuegong; Jockusch, Steffen; Franz, Roberto; Washington, Ilyas; Adam, Waldemar; Bosio, Sara G. "Stereochemical Features of the Physical and Chemical Interactions of Singlet Oxygen with Enecarbamates." *Organic Letters*, **2003,** vol. 5 No. 26, 4951-4953

(15) Criegee, Rudolf. Mechanisum of Ozynolysis, *Angew. Chem. Internat. Edit.* **1975,** vol. 14, no.11, 745-752

(16) Poon, T; Park, S.H.; Elemes, Y.: Foote, C.S. "Reaction of N-Substituted 1,2,4-Triazoline-3,5-diones and trans-Cyclooctene. Direct observations of an Aziridinium imide." *J. Am. Chem. Soc.* **1995** 17, 10468.

(17) Poon, T. Personal communication.